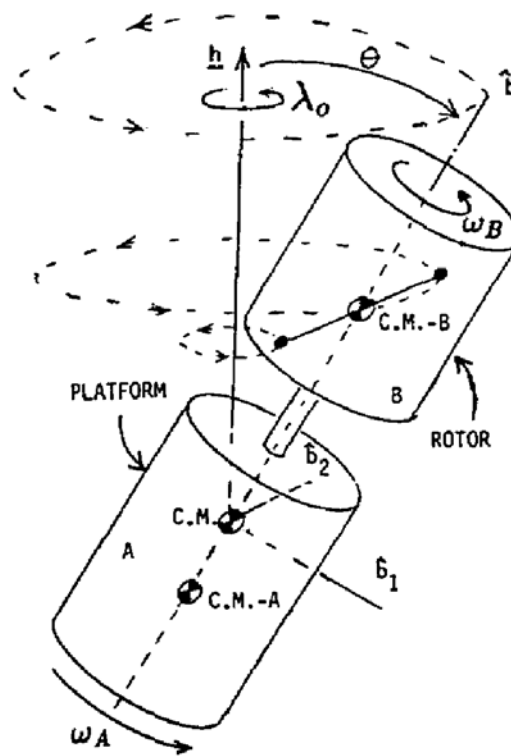


Nonlinear Control Systems

Course Project

Dual Spin Spacecraft

Final Report



Author: Ramin Mehran

Student Number: 821315102

Lecturer: Dr. Taghirad

Fall 2004

Part 1

System Modeling

1-0 Introduction

The control problem involving dual-spin spacecraft is concerned with reducing nutation that becomes excited during spin-up[1]. The interaction between spin and nutation has been modeled by mean of the rotational translational actuator with translational oscillator where translation represents nutation [1]. The interaction between rotation and translation in the transitional oscillator is analogous to the interaction between spin and nutation in dual-spin spacecraft. Thus, we will investigate the modeling and nonlinear control of the it, shown in Figure 1, as our benchmark to study nonlinear systems [2] and [3]

The rotational translational actuator with translational oscillator shown in Figure 1 consists of an unbalanced point mass of m mounted on a device with inertia I which the whole is called proof mass ($p.m$). In addition, the $p.m$ is riding on a cart constrained to move horizontally and. The moving card is attached to a wall by a spring with spring constant k . Let M denote the total mass of proof mass, and let e denote the length of the proof mass. It should be noted that gravitational effects is considered by this modeling. Let q denote the transitional position of the center of the dist from its equilibrium position, and let θ denote the counter-clockwise rotational angle of the $p.m$ where $\theta = 0$ corresponds to a 90-degree rotation from the spring axis as shown in Figure 1. Let N denote the control torque applied to the $p.m$ and let F denote the output force applied to the moving cart.

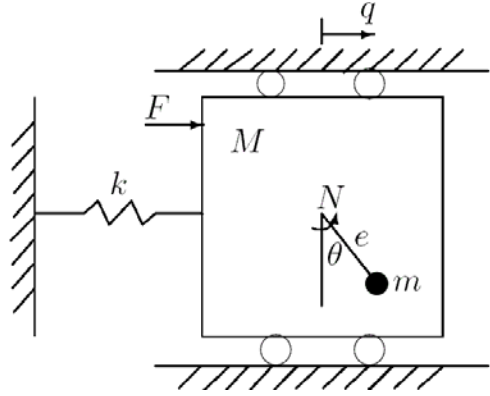


Figure 1. Rotational actuator to control a translational oscillator

1 - State-Space Equations and Equilibrium Points

Dynamic equation of the system in Figure 1 is given by

$$(M + m)\ddot{q} + kq = -me(\ddot{\theta} \cos \theta - \dot{\theta}^2 \sin \theta) + F \quad \text{Eq. 1}$$

$$(I + me^2)\ddot{\theta} = -me\ddot{q} \cos \theta + N \quad \text{Eq. 2}$$

To construct the state space equations we will consider variables give by

$$\begin{cases} x_1 = q \\ x_2 = \dot{q} \\ x_3 = \theta \\ x_4 = \dot{\theta} \end{cases} \quad \text{Thus, } x_2 = \dot{x}_1 \text{ and } x_4 = \dot{x}_3 \quad \text{Eq. 3}$$

and by substituting the new variables into Eq. 1 and Eq. 2 we obtain state space equations:

$$\begin{cases} \dot{x}_1 = x_2 \\ \dot{x}_2 = Gx_1 + Hx_2^2 + Rx_2 + Pu_1 \\ \dot{x}_3 = x_4 \\ \dot{x}_4 = QGx_1 + QHx_2^2 + QPu_1 + [QR + P]u_2 \end{cases} \quad \text{Eq. 4}$$

$$Q = \frac{-me}{I + me^2} \cos(x_3), G = \frac{-k}{M + m + Q \cos(x_3)}, H = \frac{mesin(x_3)}{M + m + Q \cos(x_3)}, P = \frac{1}{I + me^2}, R = \frac{G}{k}$$

By setting $\dot{X} = \underline{0}$ in Eq. 4, and by neglecting the inputs u_1 and u_2 , we obtain the equilibrium points as

$$X^* = \begin{pmatrix} 0 \\ 0 \\ x_3^* \\ 0 \end{pmatrix}, \text{ where } x_3^* \text{ is an arbitrary angle} \quad \text{Eq. 5}$$

1-2 Linearization and Stability Discussion

The process of linearization consists of taking the derivative of the state space function $f(x)$ with respect to state variables at the neighborhood of the equilibrium points, substituting the equilibrium point values in the equations and shifting the variables so that the equilibrium point is placed at the origin. The state equations in Eq. 4 could be equivalently considered as

$$\dot{X} = f(X) + g(x)u \quad \text{Eq. 6}$$

where it is ready to calculate the derivatives (Jacobian matrix) for linearization.

$$\text{Jacobian} = J(X) = \left[\frac{\partial f_i}{\partial x_{ij}} \right]_{i=1..4} \quad \text{and} \quad A = J(X^*) \quad \text{Eq. 7}$$

where X^* is the equilibrium point and A is the resultant state matrix.

Thus, we have

$$J(X) = \begin{bmatrix} 0 & 1 & 0 & 0 \\ G & 0 & \frac{\partial H}{\partial x_3} & 2x_4 H \\ 0 & 0 & 0 & 1 \\ QG & 0 & Q \frac{\partial H}{\partial x_3} & 2x_4 QH \end{bmatrix} \quad \text{Eq. 8}$$

and by the fact that the equilibrium is at the origin, the A matrix is simplified to

$$A = \begin{bmatrix} 0 & 1 & 0 & 0 \\ \frac{k}{P - (M + m)} & 0 & 0 & 0 \\ 0 & 0 & 0 & 1 \\ \frac{k.m.e}{(M + m)(I + me^2) - me} & 0 & 0 & 0 \end{bmatrix} \quad \text{Eq. 9}$$

Considering the equation Eq. 9 we could discuss about the stability of the equilibrium points in Eq. 5. Hence, the parametric eigen-values the A

might describe the behavior of the system in the near of the origin. We obtain the eigen values as

$$\lambda_{1,2} = 0, \lambda_{3,4} = \pm \sqrt{\frac{-kI}{me^2(1+m+M) + I(m+M) - me}} \quad \text{Eq. 10}$$

and therefore since the it has at least two eigen values on the imaginary axis, the linear state matrix could not be conclusive alone for stability analysis.

Since the system does not have any energy consumption, in the absence of friction and damping, we will confidently conclude that the equilibrium point at the origin is not stable in Lyapunov sense. In fact, the system oscillates infinitely and we need energy consuming parts for stability.

1-3 Non-Dimensionalized State Space Equations

By introducing the dimensionless variables in Eq. 11, the dynamic equations Eq. 1 and Eq. 2 are equivalent to the dimensionless equations Eq. 12 and Eq. 13.

$$\omega = \frac{1}{k} \sqrt{\frac{M+m}{I+me^2}} F \quad u = \frac{M+m}{k(I+me^2)} N \quad \tau = \sqrt{\frac{k}{M+m}} t \quad \xi = \sqrt{\frac{M+m}{I+me^2}} q \quad \text{Eq. 11}$$

Substituting the new variables yields

$$\ddot{\xi} + \xi = \varepsilon(\dot{\theta}^2 \sin \theta - \ddot{\theta} \cos \theta) + \omega \quad \text{Eq. 12}$$

$$\ddot{\theta} = u - \varepsilon \ddot{\xi} \cos \theta \quad \text{Eq. 13}$$

and the dimensionless state space equation of the form

$$\dot{\mathbf{x}} = \mathbf{f}(\mathbf{x}) + \mathbf{g}(\mathbf{x})u + \mathbf{d}(\mathbf{x})w \quad \text{Eq. 14}$$

where,

$$\begin{aligned}
\mathbf{f}(\mathbf{x}) &= \left(x_2 \quad \frac{-x_1 + \epsilon x_1^2 \sin x_3}{1 - \epsilon^2 \cos^2 x_3} \quad x_4 \quad \frac{\epsilon \cos x_3 (x_1 - \epsilon x_1^2 \sin x_3)}{1 - \epsilon^2 \cos^2 x_3} \right)^T \\
\mathbf{g}(\mathbf{x}) &= (0 \quad -\epsilon \cos x_3 \quad 0 \quad 1)^T / (1 - \epsilon^2 \cos^2 x_3), \\
\mathbf{d}(\mathbf{x}) &= (0 \quad 1 \quad 0 \quad -\epsilon \cos x_3)^T / (1 - \epsilon^2 \cos^2 x_3).
\end{aligned} \tag{Eq. 15}$$

and

$$\epsilon = me / \sqrt{(I + me^2)(M + m)} \text{ and } (x_1, x_2, x_3, x_4) = (\xi, \dot{\xi}, \theta, \dot{\theta}). \tag{Eq. 16}$$

However, by joining together the terms $\mathbf{g}(\mathbf{x})\mathbf{u} + \mathbf{d}(\mathbf{x})\mathbf{w}$ in Eq. 14 we in a unified term $\bar{\mathbf{g}}(\mathbf{x})\bar{\mathbf{u}}$ we could get the familiar form of Eq. 6.

1-4 Viscous Friction and Damping Ratio

By adding friction and spring damping ratio, we obtain more realistic model of the system and the dynamic equation Eq. 1 of the system will change to

$$(M + m)\ddot{q} + kq + b\dot{q} = -me(\ddot{\theta} \cos \theta - \dot{\theta}^2 \sin \theta) - c\dot{\theta} \tag{Eq. 17}$$

and from this equation alone it is obvious that the equilibrium points will not be affected since both new terms contain \dot{q} and $\dot{\theta}$. However, we will recalculate the state equations for Eq. 17, which is very similar to Eq. 4.

$$\begin{cases}
\dot{x}_1 = x_2 \\
\dot{x}_2 = Gx_1 + \frac{G}{K}bx_2 + \frac{G}{k}cx_4 + Hx_4^2 - Ru_2 + Pu_1 \\
\dot{x}_3 = x_4 \\
\dot{x}_4 = QGx_1 + \frac{QG}{K}bx_2 + \frac{QG}{K}cx_5 + QHx_4^2 + QPu_1 + [QR + P]u_2
\end{cases} \tag{Eq. 18}$$

$$Q = \frac{-me}{I + me^2} \cos(x_3), G = \frac{-k}{M + m + Q \cos(x_3)}, H = \frac{me \sin(x_3)}{M + m + Q \cos(x_3)}, P = \frac{1}{I + me^2}, R = \frac{G}{k}$$

Let $\dot{\mathbf{X}} = \mathbf{0}$ in Eq. 18 we get the same equilibrium points as in Eq. 4 since the $\dot{x}_1 = x_2 = 0$ condition eliminated the newly added terms. Thus, the equilibrium points are intact. However, the new terms provide the

stability properties for the equilibrium points (asymptotically). The new state space equations are

$$\begin{cases} \dot{x}_1 = x_2 \\ \dot{x}_2 = \frac{-me \cos(x_1)[-kx_3 + mex_2^2 \sin(x_1) - (b+c)x_4]}{a} + \frac{(M+m)u}{a} \\ \dot{x}_3 = x_4 \\ \dot{x}_4 = \frac{[-kx_3 + mex_2^2 \sin(x_1) - (b+c)x_4](I+me^2)}{a} - \frac{me \cos(x_1)u}{a} \end{cases} \quad \text{Eq. 19}$$

$$a = (M+m)(I+me^2) - me^2 \cos^2(x_1)$$

186 N/m	K	1 kg	M
0.15	c	0.1 kg	m
0.99	b	0.06 m	e
		$2 \text{ kgm}^{-4} 10 \times 2.2$	I

Figure 2. System paramters

$\Delta m = \pm 10\%$
$\Delta M = \pm 10\%$
$\Delta K = \pm 1\%$
$\Delta I = \pm 1\%$
$\Delta q_0 = \pm 5cm$

Figure 3. System Uncertainties

Special note:

The system exhibits the resonance capture phenomenon, which is when trying to spin-up the rotational proof mass to a desired angular speed: if the available torque isf limited in magnitude, the mass cab be spun up only to the angular speed $\sqrt{k/(M+m)}$ which corresponds to the natural frequency of the translational oscillator. Avoiding this capture is a challenging control problem [6].

Part 2

Feedback Linearization

2-0 Introduction

In this section we will recall the results of the last report about feedback linearization of our benchmark problem. We first introduce a state transformation that will help us to in feedback linearization design and then we show that this new state space equation is input-state feedback linearizable. We construct a stabilizing feedback for the linearized system in this framework and enforce the error to have specific dynamic. In addition, by considering $y=\theta$ as system output, we show that the system is input-output feedback linearizable with stable zero dynamics. We present the linearizing feedback law and the tracking controller.

2-1 State Transformation

The system in its early form in Section 1-3 is not input-state linearizable, since it does not satisfy the insolubility condition according to [4]. But with a tricky transformation of states we could have a state space system which is input-state feedback linearizable.

With state Transformation

$$X_1 = q + \varepsilon \sin(\theta), X_2 = \dot{X}_1, X_3 = \theta, X_4 = \dot{\theta}, \varepsilon = \frac{me}{M+m} \quad \text{Eq. 20}$$

we derive new state space equations

$$\begin{cases} \dot{X}_1 = X_2 \\ \dot{X}_2 = \frac{-k(x_1 - \varepsilon \sin x_3) + F}{M+m} \\ \dot{X}_3 = X_4 \\ \dot{X}_4 = \frac{k\varepsilon(x_1 - \varepsilon \sin x_3) \cos x_3 - me\varepsilon x_4^2 \sin x_3 \cos x_3 - F\varepsilon \cos x_3 + N}{I + me^2 - me\varepsilon \cos^2 x_3} \end{cases} \quad \text{Eq. 21}$$

2-2 Input-State Feedback Linearization

Considering the above state space we have shown in the last report that the system involutive by satisfying the condition in the remarks of page 235 of [8]. With zero disturbance we have

$$\begin{cases} \dot{X}_1 = X_2 \\ \dot{X}_2 = \frac{-k(x_1 - \varepsilon \sin x_3)}{M + m} \\ \dot{X}_3 = X_4 \\ \dot{X}_4 = \frac{k\varepsilon(x_1 - \varepsilon \sin x_3) \cos x_3 - me\varepsilon x_4^2 \sin x_3 \cos x_3 + N}{I + me^2 - me\varepsilon \cos^2 x_3} \end{cases}$$

And we introduce dephomorphism as

$$\begin{cases} z_1 = x_1 \\ z_2 = x_2 \\ z_3 = \frac{-k(x_1 - \varepsilon \sin x_3)}{M + m} \\ z_4 = \frac{-k(x_2 - \varepsilon x_4 \cos x_3)}{M + m} \end{cases}, \text{ where } \varphi(x) = Z$$

and this lead us to

$$\begin{cases} \dot{z}_1 = z_2 \\ \dot{z}_2 = z_3 \\ \dot{z}_3 = z_4 \\ \dot{z}_4 = \frac{-k(\dot{x}_2 + \varepsilon x_4^2 \sin x_3 - \varepsilon x_4 \cos x_3)}{M + m} \end{cases}$$

and thus we have

$$\frac{-k}{M + m} \left[\frac{-k(x_1 - \varepsilon \sin x_3)}{M + m} + \varepsilon x_4^2 \sin x_3 - \varepsilon \cos x_3 \left[\frac{k\varepsilon(x_1 - \varepsilon \sin x_3) \cos x_3 - me\varepsilon x_4^2 \sin x_3 \cos x_3 + N}{I + me^2 - me\varepsilon \cos^2 x_3} \right] \right] \quad \text{Eq. 22}$$

where N is the controller signal and v is the output of linear controller.

$$\begin{cases} \dot{z}_1 = z_2 \\ \dot{z}_2 = z_3 \\ \dot{z}_3 = z_4 \\ \dot{z}_4 = v \end{cases} \quad \text{Eq. 23}$$

In order to have $(s+I)^4$ dynamic for error, we should have a state space feedback $K = [1, 4, 6, 4]$ and hence,

$$v = -z_1 - 4z_2 - 6z_3 - 4z_4$$

which is equal to

$$v = \left(\frac{6k}{M+m} - 1\right)x_1 + \left(\frac{4k}{M+m} - 4\right)x_2 - \frac{6k_4}{M+m} \sin(x_3) - \frac{4k_4}{M+m} x_4 \cos x_3 \quad \text{Eq. 24}$$

And finally the nonlinear controller $u(x, v)$ will be

$$u(x, v) = N = \alpha(x) + \beta(x)v$$

where,

$$\alpha(x) = -\frac{L_f^4 z_1}{L_g L_f^{n-1} z_1}, \beta(x) = \alpha(x) = -\frac{1}{L_g L_f^{n-1} z_1}$$

2-3 Input-Output Linearization

We have shown that the system is input output linearizable with relative degree $r=2$ and bounded zero-dynamics which is actually oscillatory.

Recalling state equations

$$f(x) = \begin{bmatrix} x_2 \\ \frac{-x_1 + \varepsilon x_4^2 \sin x_3}{1 - \varepsilon^2 \cos^2 x_3} \\ x_4 \\ \frac{\varepsilon \cos x_3 (x_1 - \varepsilon x_4^2 \sin x_3)}{1 - \varepsilon^2 \cos^2 x_3} \end{bmatrix}, g(x) = \begin{bmatrix} 0 \\ \frac{-\varepsilon \cos x_3}{1 - \varepsilon^2 \cos^2 x_3} \\ 0 \\ \frac{1}{1 - \varepsilon^2 \cos^2 x_3} \end{bmatrix}$$

we have

$$\ddot{y} = \ddot{\theta} = \dot{x}_4 = \frac{\varepsilon \cos(x_3)x_1 - \varepsilon^2 \sin(x_3)\cos(x_3)x_4^2}{1 - \varepsilon^2 \cos^2(x_3)} + \frac{1}{1 - \varepsilon^2 \cos^2 x_3} u$$

yields

$$\mu_1 = x_3$$

$$\mu_2 = \dot{x}_3 = x_4$$

and

$$L_g \psi = 0$$

$$\Rightarrow \frac{\partial \psi}{\partial x_4} \left(\frac{1}{1 - \varepsilon^2 \cos^2 x_3} \right) + \frac{\partial \psi}{\partial x_2} \left(\frac{-\varepsilon \cos x_3}{1 - \varepsilon^2 \cos^2 x_3} \right) = 0$$

Yields

$$\psi_1 = x_1$$

$$\frac{\partial \psi}{\partial x_4} + \frac{\partial \psi}{\partial x_2} (-\varepsilon \cos x_3) = 0$$

which we could choose

$$\psi_2 = x_4 \varepsilon \cos x_3 + x_2$$

as a possible solution. Hence we have

$$\begin{cases} \dot{\mu}_1 = \mu_2 \\ \dot{\mu}_2 = v \\ \psi_1 = x_1 = x_2 \\ \psi_2 = x_4 \varepsilon \cos x_3 - x_4 x_3 \varepsilon \sin(x_3) + x_2 \end{cases}$$

and the controller is

$$u = \frac{1}{L_g L^{r-1} f h} (-L^r f h + v)$$

Thus, the normal form equations become

$$\begin{cases} \dot{\mu}_1 = \mu_2 \\ \dot{\mu}_2 = v \\ \dot{\psi}_1 = \psi_2 - \mu_2 (\varepsilon \cos \mu_1) \\ \dot{\psi}_2 = \frac{\varepsilon^2 \cos^2(\mu_1) \psi_1 - \varepsilon^3 \sin(\mu_1) \cos^2(\mu_1) - \psi_1 + \varepsilon \sin(\mu_1) \mu_2^2}{1 - \varepsilon^2 \cos^2(\mu_1)} - \mu_2^2 \varepsilon \sin \mu_1 \end{cases} \quad \text{Eq. 25}$$

And the zero dynamics are

$$\begin{cases} \dot{\psi}_1 = \psi_2 \\ \dot{\psi}_2 = -\psi_1 \end{cases}$$

which is obviously oscillatory but bounded with limited energy. Thus we conclude that the system is input-output linearizable with stable zero dynamics in Lyapunov sense.

For tracking purpose we have simply used the control law

$$u = \frac{1}{L_g L_f^{-1} \mu_1} [-L_f^2 \mu_1 + \ddot{y}_d - 2\tilde{\mu}_2 - \tilde{\mu}_1], \text{ where } y_d = \sin(2t) \text{ and } \tilde{\mu}_i = \mu_i(t) - \mu_{i,d}$$

The detailed discussion and control law formulas are presented in last report and we end describing the design here, and we will present the simulation and the conclusive remarks of the feedback linearization in the next section.

Input-State Feedback Linearization (1 4 2

Regulator

10

M,m,e,I,k

:
.1

[0,0,0.001,0]

[0.1,0,0.001,0]

.2

4

4

[-120.5434,-0.0284 + 2.3093i,-0.0284 - 2.3093i,-1.3998] :

[1 122 181 660 900] :

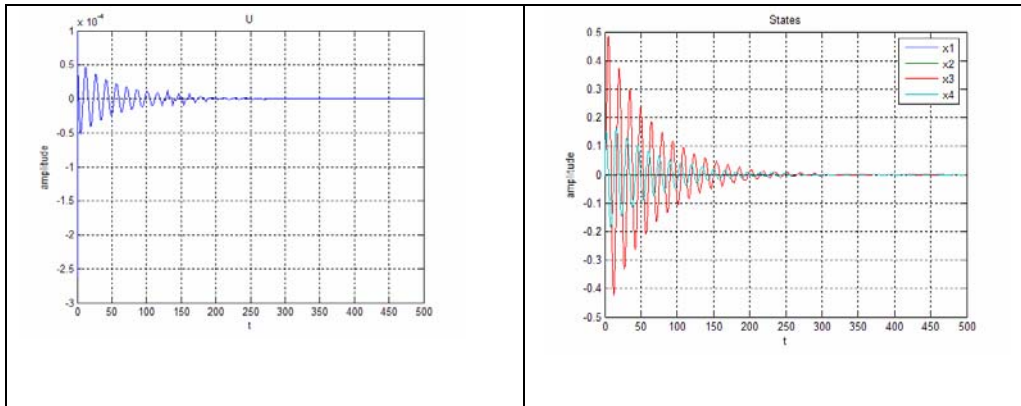
10

.3

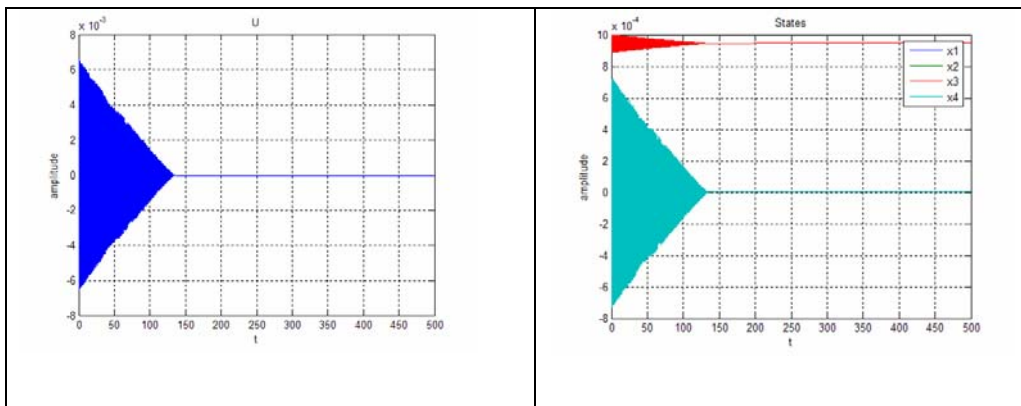
Model-based

(!).

.4

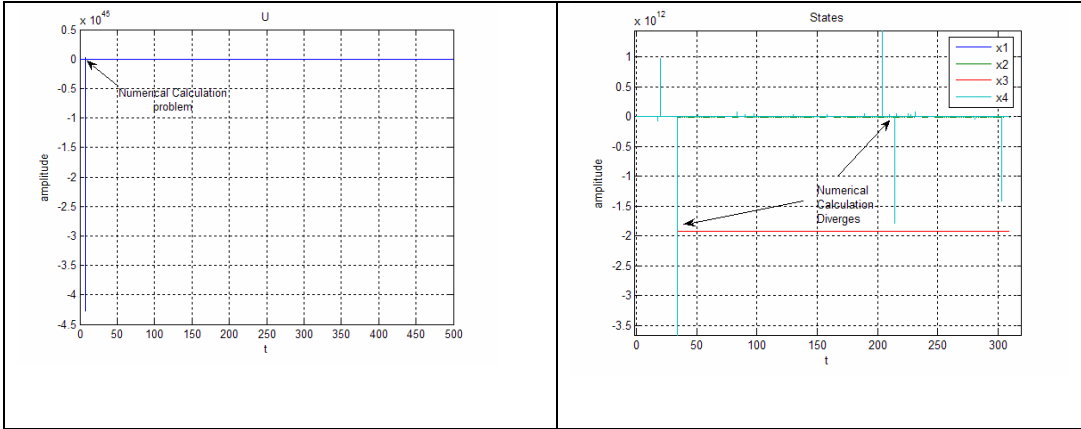


1 4 2



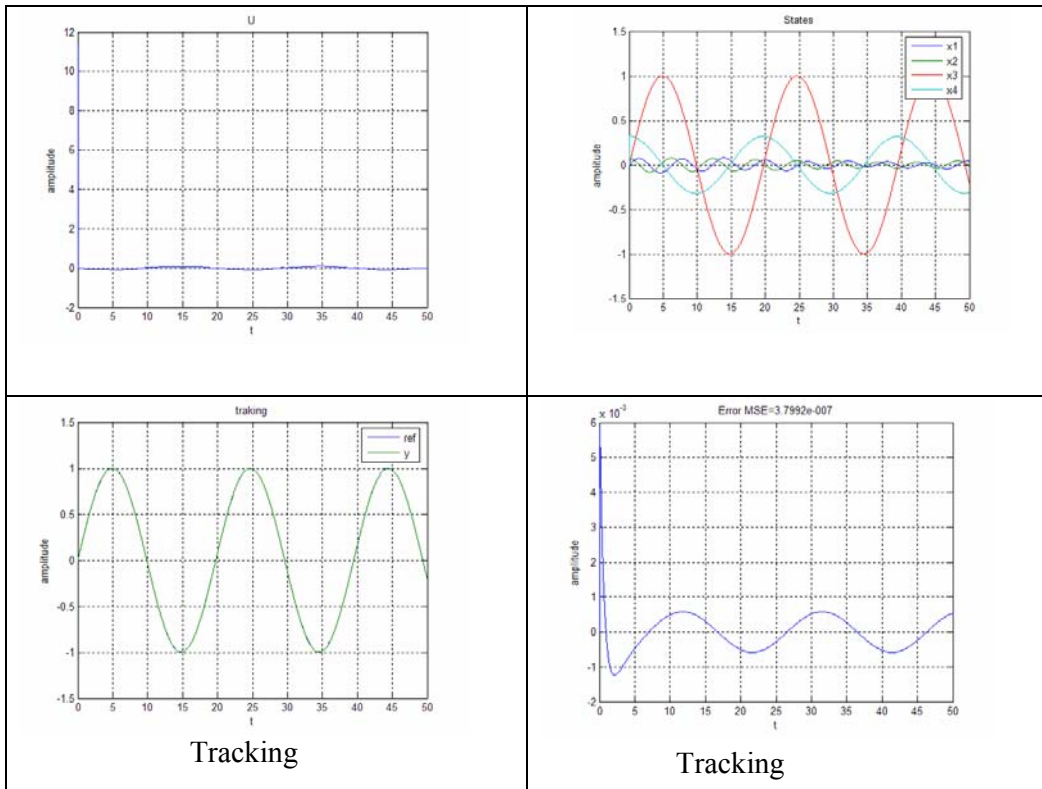
10

- 1 4 2

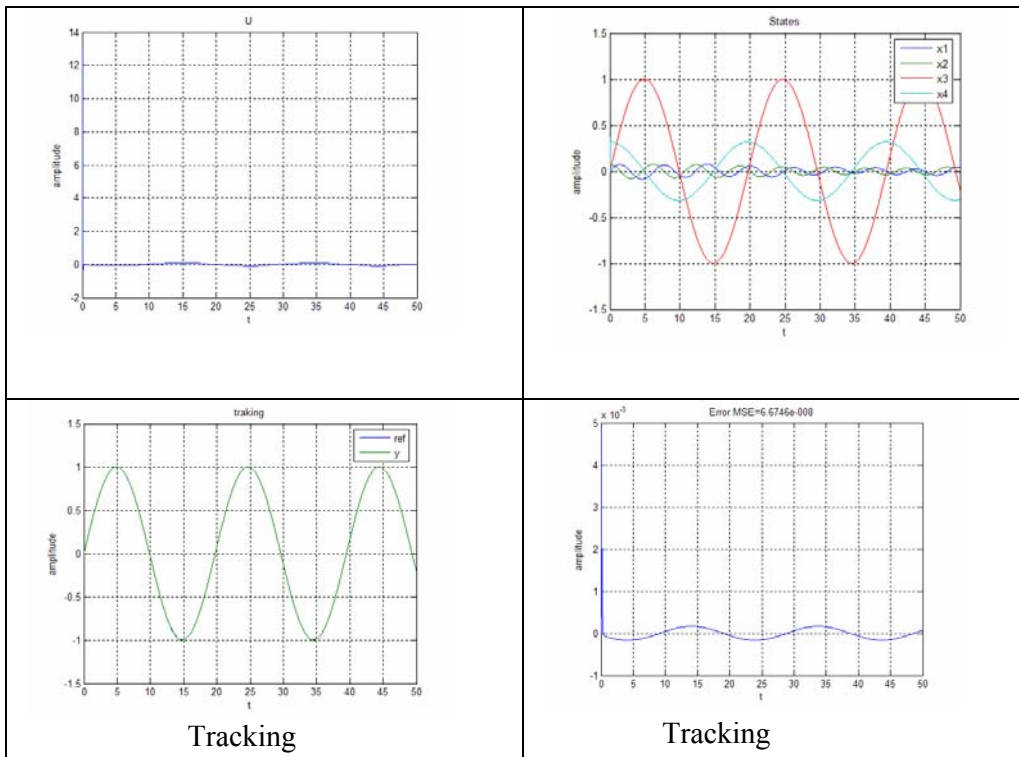


:

- 1 4 2

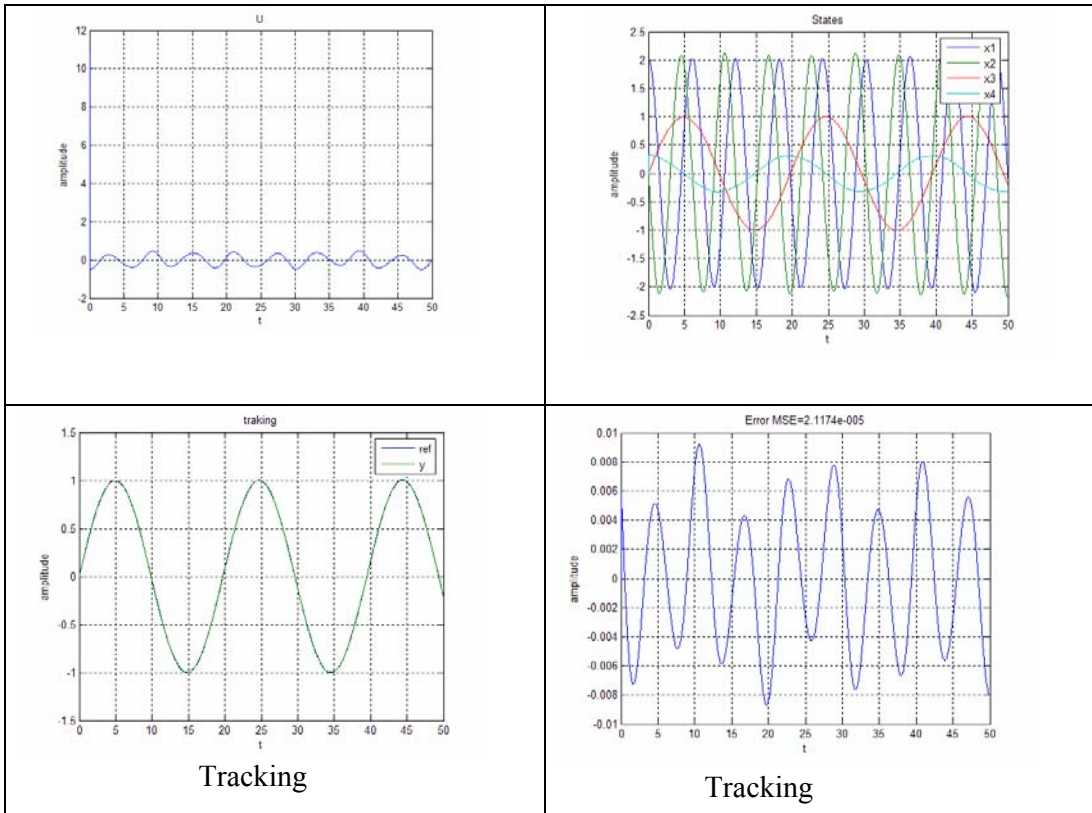


2 4 2



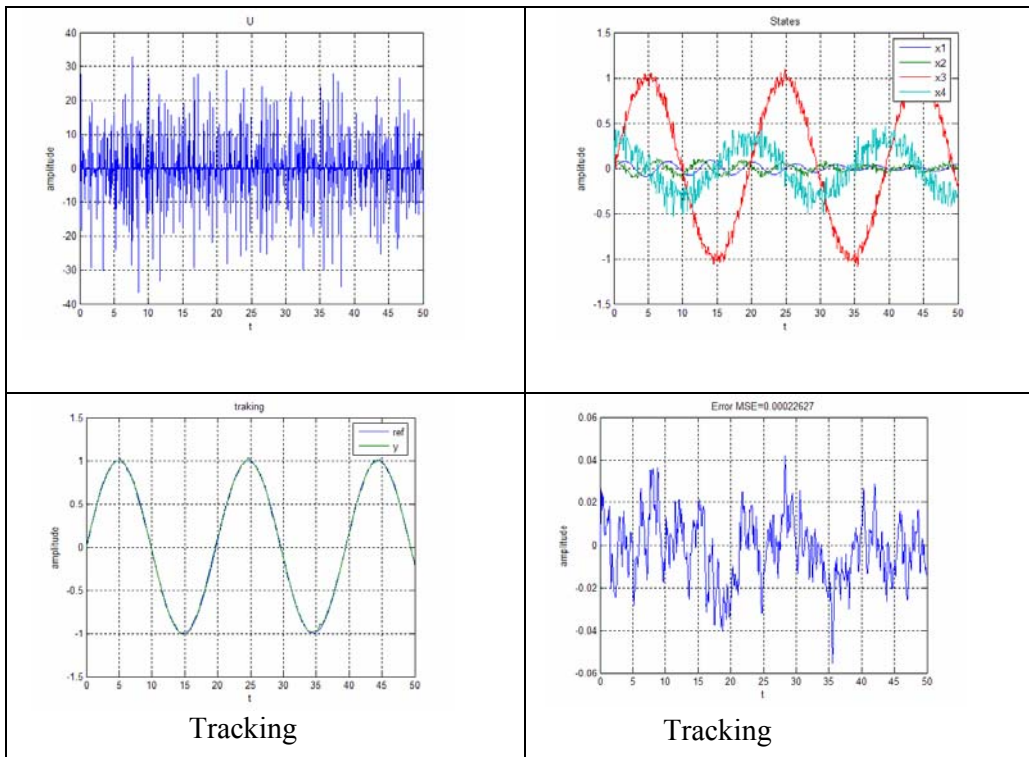
$k=[12 \ 36]$

2 4 2

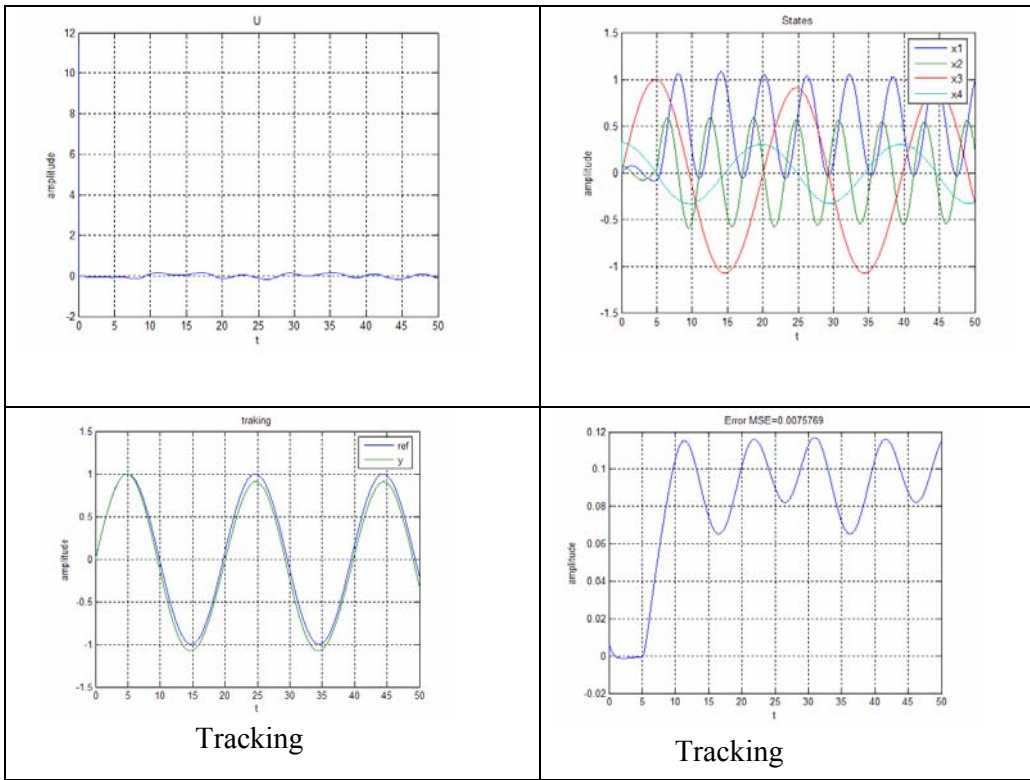


10

2 4 2



- 2 4 2



() $w=0.5u(t-5)$ - 2 4 2

50

- Tracking

<i>MSE</i>	
3.799×10^{-7}	.1
6.674×10^{-8}	.2
2.117×10^{-5}	10 .3
2.226×10^{-4}	.4
7.576×10^{-3}	.5

Part 3

Backstepping And Sliding Mode Control

3-0 Introduction

In this part we will discuss the design of Backstepping and Sliding mode controllers our benchmark problem. For the Backstepping controller, we consider the transformation of variables as in Section 1-3 plus new state variables in the Section 2-1. This choice of state variables will facilitate the design in the backstepping steps. In the Sliding mode control design we have considered we used original state variables.

3-1 Backstepping Design

Backstepping, introduced in 1990s is a recursive design for systems with nonlinearities not constrained by linear bounds. The true potential of backstepping was discovered only when this approach was developed for nonlinear system with structured uncertainty. With adaptive backstepping, global stabilization in the presence of unknown parameters is achieved and with robust backstepping, we could achieve it in presence of disturbances. Backstepping easily handles uncertainties and unknown parameters, and this was the reason for rapid popularity and acceptance[5]. Unlike feedback linearization, backstepping can avoid the cancellation of useful nonlinearities. So, it offers the prospect of a more practicable nonlinear control. In addition, backstepping is a flexible controller design, which allows the designer to choose not only values of gains, but also the form of intermediate nonlinear terms and even of Lyapunov functions, in order to customize the closed-loop system response to meet the required specifications[6].

a. Literature Review

In this section we intend to design a backstepping controller for the dual spin space craft model, which is a well-known benchmark problem. We

have done some literature reviews regarding this special problem and found some highly related works in this field. [1] considers the stabilization and disturbance attenuation objectives for our benchmark problem. This goal has been achieved by using a passive absorber and in [3]**Error! Reference source not found.**, with similar results, a passivity-based controller is designed. However, the main objective of the most of the works was on designing a stabilizing controller with deference controller designs including backstepping. In **Error! Reference source not found.**, an integrator backstepping controller has been design and compared to a partial feedback linearization design for the dual spin space craft problem. The results in **Error! Reference source not found.** are very intuitive and helpful for creating our backstepping controller. At last but not least, we found a significantly helpful IEEE paper which has solved the problem of designing a tracking controller for our system [7]. This very paper guided us to discover a more comprehensive study on this benchmark problem with design of backstepping controller in [6]¹. Considering the strong design and comprehensiveness of the discussions in **Error! Reference source not found.**, we decided to build our design on the basis of this work by adding some modifications the original work only. Thus, the backstepping design procedure we will discuss in the following section will be the same as in **Error! Reference source not found.** and we will clarify the our modifications in place.

b. Choosing a Suitable Model

To satisfy the need for a suitable model of state variables we first switched to the dimensionless co-ordinates of [1],

¹ It should be noted that this is not an IEEE paper and if it would be stated in other reports as a one it is a false claim. This is published on IJRNC (1998) and I found it on the net but I had problems for downloading this from Internet, since it was a John Wiley publication. Hence, I decided to ask some friend in US universities to download it for me. The PDF file of this paper is provided along with this report.

$$(1 - \varepsilon^2 \cos^2 \theta) \ddot{\xi} + \xi = \varepsilon(\dot{\theta}^2 \sin \theta - \cos \theta u) + w \quad \text{Eq. 26}$$

$$(1 - \varepsilon^2 \cos^2 \theta) \ddot{\theta} = \varepsilon \cos \theta (\xi - \varepsilon \dot{\theta}^2 \sin \theta \cos \theta) + u \quad \text{Eq. 27}$$

which, are the same as co-ordinates of Section 1-3. This is called *dimensionless* because they do not change the dimensions of the state variables. However, the very important point to note is that this transformation scales the time variable and this modification should be considered in frequency analysis of the closed-loop system. This scaling procedure is done also on the u and w and it should be considered in facing with uncertainties.

The backstepping design of **Error! Reference source not found.** guided us to choose a the same coordinates which are also the same as in Section 2-1. Thus, to obtain the cascade form suitable for backstepping the change of coordinates

$$x_1 = \xi + \varepsilon \sin \theta, \quad x_2 = \dot{\xi} + \varepsilon \dot{\theta} \cos \theta, \quad x_3 = \theta, \quad x_4 = \dot{\theta} \quad \text{Eq. 28}$$

and the feedback

$$u = (1 - \varepsilon^2 \cos^2 \theta)v - (\varepsilon \dot{\xi} \cos \theta - \varepsilon^2 \dot{\theta}^2 \cos \theta \sin \theta) \quad \text{Eq. 29}$$

results

$$\dot{x}_1 = x_2$$

$$\dot{x}_2 = -x_1 + \varepsilon \sin x_3 + w$$

$$\dot{x}_3 = x_4$$

$$\dot{x}_4 = v$$

Eq. 30

The Eq. 30 is all ready for a backstepping design and the only step remained for building a tracking system is to define reference signals for all states x_1 - x_4 . As we know the basic backstepping is a stabilization

method and to handle tracking we should convert the tracking problem to a stabilization problem. Thus, we will implicitly design a backstepping stabilizing controller for new state variables similar to $z_i = x_i - x_{iref}$, which are errors. To do so, we need to calculate analytically the reference signals for the state variables when the output signal is $y = \theta = x_3$. One of main differences between our control design and the controller in **Error! Reference source not found.**, is the choice system output for tracking, which is the transitional displacement in **Error! Reference source not found.** and mass rotational angle in our experiment. In **Error! Reference source not found.**, all of reference state variables are calculated analytically by considering $\xi_{ref} = A_r \sin \omega_r t$. In our design, the trivial answer for the reference of third and fourth state variables is $x_{3ref} = \theta_{ref} = y_d$, $x_{4ref} = \dot{\theta}_{ref} = \dot{y}_d$. However, the analytical calculation of the rest of state variables is a cumbersome task. Thus we decided to calculate these reference signals at each time step using nonlinear system dynamics. For reference signals, Eq. 26 yields

$$\ddot{\xi}_{ref} + \xi_{ref} = -\varepsilon \frac{d^2}{dt^2} \sin \theta_{ref} \quad \text{Eq. 31}$$

which could be solved numerically in MATLAB. Thus, in each time interval we have calculated the reference signals and we obtain

$$\begin{aligned} x_{1ref} &= \xi + \varepsilon \sin \theta_{ref} \\ x_{2ref} &= \dot{\xi} + \varepsilon \dot{\theta}_{ref} \cos \theta_{ref} \\ x_{3ref} &= \theta_{ref} \\ x_{4ref} &= \dot{\theta}_{ref} \end{aligned} \quad \text{Eq. 32}$$

and now we are all ready for backstepping design.

c. Backstepping Design Steps

Four state variables require us to design the backstepping controller in four steps. Since the design steps are the same as in **Error! Reference source not found.**, we will only represent the results and avoid detailed

calculation of control variables here. Instead we will emphasize on the concepts and special considering of our system.

Step 1: We introduce the error variable

$$z_1 = x_1 - x_{1ref} \quad \text{Eq. 33}$$

and calculating the derivative yields

$$\dot{z}_1 = x_2 - x_{2ref} \quad \text{Eq. 34}$$

We view x_2 as the virtual control in Eq. 34 and we introduce the error variable as $z_2 = x_2 - \alpha_1$, where α_1 is the first stabilizing function and we will design it to obtain satisfactory stabilizing behavior in Lyapunov sense. Representing the Lyapunov function

$$V_1 = \frac{1}{2}z_1^2 \quad \text{Eq. 35}$$

will help us to control the error of the first state variable and preserves the boundedness of that state. Computing the time derivative of the V_1 yields

$$\begin{aligned} \dot{V}_1 &= z_1 \dot{z}_1 \\ &= z_1(\alpha_1 + z_2 - x_{2ref}) \end{aligned} \quad \text{Eq. 36}$$

Thus, the choice of

$$\alpha_1 = -c_1 z_1 + x_{2ref} \quad \text{Eq. 37}$$

ensures that when $z_2 = 0$, $\dot{V}_1 = -c_1 z_1 + z_2$ is negative definite in z_1 . c_1 is a positive constant which is a design parameter. In addition, we obtain

$$\dot{z}_1 = -c_1 z_1 + z_2 \quad \text{Eq. 38}$$

Step 2: To guaranty the stability of the first Lyapunov function, we state that $z_2 \rightarrow 0$. Therefore, we introduce a new Lyapunov function in this step as

$$V_2 = \frac{1}{2}(z_1^2 + z_2^2) \quad \text{Eq. 39}$$

Then we rewrite \dot{z}_2 as

$$\dot{z}_2 = -z_1 + \varepsilon(\sin x_3 - \sin x_{3ref}) + c_1 z_2 - c_1^2 z_1 + w \quad \text{Eq. 40}$$

In this equation, we view $\sin x_3$ as the virtual control. This is a departure from usual backstepping designs which only employ state variables as virtual controls. In this case, however, this simple modification is not only dictated by the structure of the system, but it also yields significant improvements in closed-loop system response **Error! Reference source not found.** Thus, the new error variable is

$$z_3 = \sin x_3 - \alpha_2, \quad \text{Eq. 41}$$

and α_2 is the second stabilizing function yet to be determined by Lyapunov analysis. We replace $\sin x_3$ in Eq. 40 with $z_3 + \alpha_2$ and then we calculate derivative of V_2 as

$$\begin{aligned} \dot{V}_2 \\ = -c_1 z_1^2 - c_2 z_2^2 + \varepsilon z_2 z_3 + z_2 [c_2 z_2 + \varepsilon(\alpha_2 - \sin x_{3\text{ref}}) + c_1 z_2 - c_1^2 z_1] + z_2 w \end{aligned} \quad \text{Eq. 42}$$

Thus, choosing

$$\alpha_2 = \sin x_{3\text{ref}} + \frac{1}{\varepsilon} [c_1^2 z_1 - (c_1 + c_2) z_2] \quad \text{Eq. 43}$$

yields

$$\dot{V}_2 = -c_1 z_1^2 - c_2 z_2^2 + \varepsilon z_2 z_3 + z_2 w \quad \text{Eq. 44}$$

Hence, when $z_3=0$ we have $\dot{V}_2 = -c_1 z_1^2 - c_2 z_2^2$ and therefore we should have $z_3 \rightarrow 0$ in the next step.

The tricky choice of virtual control in this step is has positive effect on the overall controller design. **Error! Reference source not found.** has elaborated well on this property and states that the resulting controller will be free from the winding problem, since $\sin x_3$ is a periodic function of x_3 . The controller will attempt to asymptotically regulate $\sin x_3$ to zero, but will not be able to distinguish between $x_3=0$ and $2n\pi$, where n is an integer. In this way, the controller will drive x_3 to either $x_3=2n\pi$ or $(2n+1)\pi$ which are both open-loop-stable.

Step 3: Similarly, we design the stabilizing function α_3 in this step.

Taking derivative of Eq. 41 yields

$$\dot{z}_3 = x_4 \cos x_3 - \dot{\alpha}_2 \triangleq x_4 \cos x_3 - \bar{\alpha}_2 + d_2 w \quad \text{Eq. 45}$$

with $d_2 = \frac{c_1 + c_2}{\varepsilon}$ and

$$\bar{\alpha}_2 = \begin{bmatrix} \frac{\partial \alpha_2}{\partial x_{3\text{ref}}} & \frac{\partial \alpha_2}{\partial z_1} & \frac{\partial \alpha_2}{\partial z_2} \end{bmatrix} \begin{bmatrix} x_{4\text{ref}} \\ -c_1 z_1 + z_2 \\ -c_2 z_2 - z_1 + \varepsilon z_3 \end{bmatrix} \quad \text{Eq. 46}$$

Similarly, we use $x_4 \cos x_3$ as the virtual control, in what might seem as yet another unconventional choice. We define

$$z_4 = x_4 \cos x_3 - \alpha_3 \quad \text{and} \quad \dot{z}_3 = \alpha_3 + z_4 - \bar{\alpha}_2 + d_2 w. \quad \text{Thus, the third}$$

Lyapunov function will be $V_3 = \frac{1}{2}(z_1^2 + z_2^2 + z_3^2)$ and the derivative become

$$\dot{V}_3 = -c_1 z_1^2 - c_2 z_2^2 + z_3(\alpha_3 + \varepsilon z_2 - \bar{\alpha}_2) + z_3 z_4 + z_2 w + d_2 z_3 w \quad \text{Eq. 47}$$

Therefore, choosing

$$\alpha_3 = \bar{\alpha}_2 - c_3 z_3 - \varepsilon z_2 \quad \text{Eq. 48}$$

will yields

$$\dot{V}_3 = -c_1 z_1^2 - c_2 z_2^2 - c_3 z_3^2 + z_3 z_4 + z_2 w + d_2 z_3 w \quad \text{Eq. 49}$$

And

$$\dot{z}_3 = -c_3 z_3 + z_4 - \varepsilon z_2 + d_2 w \quad \text{Eq. 50}$$

Step 4: Similar to the last three steps we introduce a new Lyapunov function to include error variable z_4 as

$$V = \frac{1}{2}(z_1^2 + z_2^2 + z_3^2 + z_4^2) \quad \text{Eq. 51}$$

This is our overall Lyapunov function for the backstepping design and the rest of calculations are similar as before. We define

$$\dot{z}_4 = v \cos x_3 - x_4^2 \sin x_3 - \dot{\alpha}_3 \triangleq v \cos x_3 - x_4^2 \sin x_3 - \bar{\alpha}_3 - d_3 w \quad \text{Eq. 52}$$

With

$$d_3 \triangleq -\varepsilon + \frac{(c_1^2 + c_2^2 + c_1 c_2)}{\varepsilon} + d_2(c_1 + c_2 + c_3)$$

and

$$\bar{\alpha}_3 = \begin{bmatrix} \frac{\partial \alpha_3}{\partial x_{3\text{ref}}} & \frac{\partial \alpha_3}{\partial x_{4\text{ref}}} & \frac{\partial \alpha_3}{\partial z_1} & \frac{\partial \alpha_3}{\partial z_2} & \frac{\partial \alpha_3}{\partial z_3} \end{bmatrix} \begin{bmatrix} \frac{-(\ddot{\xi}_{\text{ref}} + \dot{\xi}_{\text{ref}})}{\varepsilon \cos \theta_{\text{ref}}} - \frac{x_{4\text{ref}} (x_{4\text{ref}} \cos \theta_{\text{ref}})^2 \sin \theta_{\text{ref}}}{\cos^3 \theta_{\text{ref}}} \\ -c_1 z_1 + z_2 \\ -c_2 z_2 - z_1 + \varepsilon z_3 \\ -c_3 z_3 + z_4 - \varepsilon z_2 \end{bmatrix} \quad \text{Eq. 53}$$

Now we are ready to compute the derivative of the last Lyapunov function, where M_d indicated the upper bound of uncertainty.

$$\begin{aligned} \dot{V} &= (z_1 \dot{z}_1 + z_2 \dot{z}_2 + z_3 \dot{z}_3 + z_4 \dot{z}_4) \\ &= z_1(-c_1 z_1 + z_2) + z_2(-c_2 z_2 - z_1 + \varepsilon z_3 + w) + z_3(-c_3 z_3 + z_4 - \varepsilon z_2 + d_2 w) \\ &\quad + z_4(v \cos x_3 - x_4^2 \sin x_3 - \bar{\alpha}_3 - d_3 w) \\ &= -c_1 z_1^2 - c_2 z_2^2 - c_3 z_3^2 + z_3 z_4 + z_4(v \cos x_3 - x_4^2 \sin x_3 - \bar{\alpha}_3) + z_2 w + d_2 z_3 w - d_3 z_4 w \\ &= -c_1 z_1^2 - \frac{c_2}{2} z_2^2 - \frac{c_3}{2} z_3^2 + z_4(v \cos x_3 - x_4^2 \sin x_3 - \bar{\alpha}_3 + z_3) - \frac{c_2}{2} z_2^2 - \frac{c_3}{2} z_3^2 + z_2 w \\ &\quad + d_2 z_3 w - d_3 z_4 w \\ &\leq -c_1 z_1^2 - \frac{c_2}{2} z_2^2 - \frac{c_3}{2} z_3^2 - \frac{c_2}{2} z_2^2 + |z_2| M_d - \frac{c_3}{2} z_3^2 + |z_3| |d_2| M_d \\ &\quad + z_4(v \cos x_3 - x_4^2 \sin x_3 - \bar{\alpha}_3) + |d_3| |z_4| M_d \\ &\leq -c_1 z_1^2 - \frac{c_2}{2} z_2^2 - \frac{c_3}{2} z_3^2 + z_4(v \cos x_3 - x_4^2 \sin x_3 - \bar{\alpha}_3 + z_3) - \frac{c_2}{2} \left(|z_2| - \frac{1}{c_2} M_d \right)^2 \\ &\quad + \frac{1}{2c_2} M_d^2 + \frac{d_2^2}{2c_3} M_d^2 - \frac{c_3}{2} \left(|z_3| - \frac{d_2}{c_3} M_d \right)^2 + \frac{d_3^2}{2c_4} M_d^2 - \frac{c_4}{2} \left(|z_4| - \frac{d_3}{c_4} M_d \right)^2 + \frac{c_4}{2} z_4^2 \\ &\leq -c_1 z_1^2 - \frac{c_2}{2} z_2^2 - \frac{c_3}{2} z_3^2 + z_4 \left(v \cos x_3 - x_4^2 \sin x_3 - \bar{\alpha}_3 + z_3 + \frac{c_4}{2} z_4 \right) + d_4 M_d^2 \end{aligned} \quad \text{Eq. 54}$$

And

$$d_4 \triangleq \frac{1}{2c_2} + \frac{d_2^2}{2c_3} + \frac{d_3^2}{2c_4}$$

In the last expression it is clear that by choosing v as

$$v = (1/\cos x_3) (-c_4 z_4 - z_3 + x_4^2 \sin x_3 + \bar{\alpha}_3) \quad \text{Eq. 55}$$

We ensure that derivative of Lyapunov function will be negative in the absence of disturbance and we will discuss the necessary conditions for attunation of disturbance later.

$$\dot{V} \leq -c_1 z_1^2 - \frac{c_2}{2} z_2^2 - \frac{c_3}{2} z_3^2 - \frac{c_4}{2} z_4^2 + d_4 M_d^2 \quad \text{Eq. 56}$$

However, to avoid division by zero, we modify the control law to be

$$v = \begin{cases} \frac{1}{\cos x_3} (-c_4 z_4 - z_3 + x_4^2 \sin x_3 + \bar{\alpha}_3) & \text{for } |\cos x_3| \geq a \\ \frac{1}{a^2} \cos x_3 (-c_4 z_4 - z_3 + x_4^2 \sin x_3 + \bar{\alpha}_3) & \text{for } |\cos x_3| < a \end{cases} \quad \text{Eq. 57}$$

And derivative of Lyapunov will become

$$\dot{V} \leq \begin{cases} -c_1 z_1^2 - \frac{c_2}{2} z_2^2 - \frac{c_3}{2} z_3^2 - \frac{c_4}{2} z_4^2 + d_4 M_d^2 & \text{for } |\cos x_3| \geq a \\ -c_1 z_1^2 - \frac{c_2}{2} z_2^2 - \frac{c_3}{2} z_3^2 - \frac{c_4}{2a^2} z_4^2 \cos^2 x_3 + d_4 M_d^2 \\ + z_4 \left(1 - \frac{1}{2a^2} \cos^2 x_3 \right) (-x_4^2 \sin x_3 - \bar{\alpha}_3 + z_3) & \text{for } |\cos x_3| < a \end{cases} \quad \text{Eq. 58}$$

where, $0 < a \ll 1$ and it is chosen to be equal to 0.01 in our implementations.

d. Disturbance Attenuation

From Eq. 56 it is evident that if $c_m \|(z_1(t), z_2(t), z_3(t), z_4(t))\|^2 \geq d_4 M_d^2$ then we conclude $\dot{V} \leq 0$, where $c_m \equiv \min\{c_1, c_2/2, c_3/2, c_4/2\}$. Considering the Lyapunov function Eq. 51 we obtain that this is equivalent to $2c_m V \geq d_4 M_d^2$. Hence we have $V_{\max} \leq \{(d_4/2c_m)M_d^2, V(0)\}$, which implies that

$$\limsup_{t \rightarrow \infty} V(t) \leq \frac{d_4}{2c_m} M_d^2 \Rightarrow \limsup_{t \rightarrow \infty} \|(z_1(t), z_2(t), z_3(t), z_4(t))\| \leq \sqrt{\frac{d_4}{2c_m}} M_d \quad \text{Eq. 59}$$

where

$$\sqrt{\frac{d_4}{2c_m}} = \sqrt{\frac{1}{2c_2 c_m} + \frac{(c_1 + c_2)^2}{2\varepsilon^2 c_3 c_m} + \frac{[-\varepsilon^2 + (c_1^2 + c_2^2 + c_1 c_2) - (c_1 + c_2)(c_1 + c_2 + c_3)]^2}{2\varepsilon^2 c_4 c_m}} \quad \text{Eq. 60}$$

Hence we conclude that to achieve disturbance attenuation, it is sufficient to choose

- A large c_2 to reduce the value of $1/2c_2 c_m$,
- A larger c_3 to reduce the value of $(c_1 + c_2)^2 / 2\varepsilon^2 c_3 c_m$,
- An even larger c_4 to reduce the value of

$$\frac{[-\varepsilon^2 + (c_1^2 + c_2^2 + c_1c_2) - (c_1 + c_2)(c_1 + c_2 + c_3)]^2}{2\varepsilon^2c_4c_m}$$

Therefore by proper choose of c_1 - c_4 values we will make $\sqrt{d_4/2c_m}$ arbitrary small and then effect of disturbance on the closed-loop can be arbitrarily attenuated. Our simulations in the next section will confirm this claim.

e. Meeting the constraints

In addition to disturbance attenuation, our backstepping controller should have certain robustness to parameter uncertainty as well as optimality in the sense of frequency response. The problem of handling parameter uncertainty could be resolved by proper choose of c_1 - c_4 gains which we have chosen to be

$$\begin{cases} c_1 = 0.001 \\ c_2 = 0.002 \\ c_3 = 12.4 \\ c_4 = 14.7 \end{cases} \quad \text{Eq. 61}$$

The simulation in the next section will confirm the disturbance attenuation and robustness of our controller in respect to provided parameter uncertainty and disturbance. The gains are first hand designed, then to satisfy the requirement and they are optimized around the above values to obtain the smallest tracking error by MATLAB's Nonlinear Control Design Toolbox.

The frequency response of the controller in a nonlinear control system could be viewed as the convergence rate of the controller to the desired values. Thus, by introducing proper values of c_1 - c_4 the convergence rate is guarantied and therefore, the bandwidth would be satisfactory. The problem requires the bandwidth of the system to be at least equal to $w_b=2$ *rad/s* and we examined our designed, in the implementation section, by

measuring equivalent settling time of the system which in some sense provides the bandwidth of the system.

It should be noted that our backstepping controller is a robust control Lyapunov function which by the imposed structure we could counteract worst cases of matched uncertainties by our stepwise construction of virtual control laws **Error! Reference source not found.** To clarify this concept we will consider a simple example. Consider the system

$$\begin{aligned}\dot{x}_1 &= x_2 + w_1(x, t) \\ \dot{x}_2 &= u + w_2(x, t),\end{aligned}\tag{Eq. 62}$$

Where the uncertainties w_1 and w_2 are bounded by known functions

$$\begin{aligned}|w_1(x, t)| &\leq \Delta_1(x_1) \\ |w_2(x, t)| &\leq \Delta_2(x_1, x_2)\end{aligned}\tag{Eq. 63}$$

which are allowed to grow faster than linear, like $\Delta_1(x_1) = x_1^2$. In the Eq. 62, the uncertainty w_1 is *matched* with x_2 . This means that if x_2 were our control, it would be able to counteract the worst case of w_1 by $x_2 = \mu_1(x_1)$ and we will design the virtual control law by backstepping procedure. Thus, the parameter uncertainty is handled in the same way as disturbance attenuation.

3-2 Implementation

In this section we present the implementation results for the designed backstepping controller in presence of noise and disturbance. Basically, tracking behavior of the controller is examined for sin and step reference signals by comparing L_2 and L_∞ norms of error. In addition, we use typical initial condition and show that our controller globally asymptotically stabilizes the system. Meanwhile, we change the reference signal frequency and we will analyze the effect on control signal and tracking error. Furthermore, we investigate the power spectral

density of error and control effort when the close-loop bandwidth is changed.

a. Global Stabilization

We examine the global stabilization of our design by testing its stabilizing ability from none-zero initial condition. We set the reference signal to be zero and set a typical initial condition of

$$\begin{cases} q_0 = 0.05 \\ \dot{q}_0 = 0.003 \\ \theta = 0.1 \\ \dot{\theta} = 0.1 \end{cases}$$

where the q value is a the edge of its bound which means the worst case according to problem source.

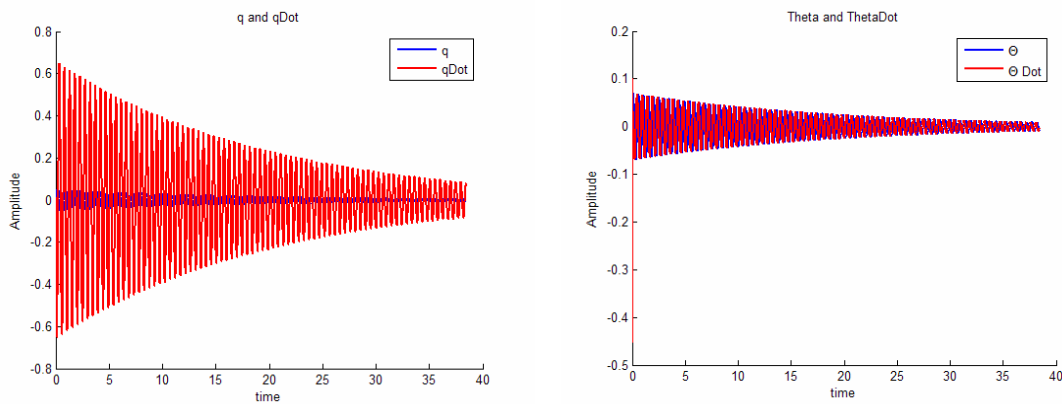


Figure 4. Global stabilizing controller – stabilizing from initial state variable [0.05, 0.003, 0.1, 0.1] (LEFT) q and \dot{q} (RIGHT) θ and $\dot{\theta}$

Figure 4 shows the stabilizing behavior of the controller from an arbitrary initial condition. Thus, we have confirmed experimentally the stabilizing behavior of the controller.

b. Tracking

If the output of the system was chosen as in **Error! Reference source not found.** it was not able to track constant signals but in this project in

have chosen $y = \theta$ thus, the reference signal could be constant as well. Here, we examine the tracking of the step and sin signals by calculating the L_2 and L_∞ norms of the tracking error. First, we set the initial state to zero and analyze the tracking behavior, and then we investigate the non-zero initial states.

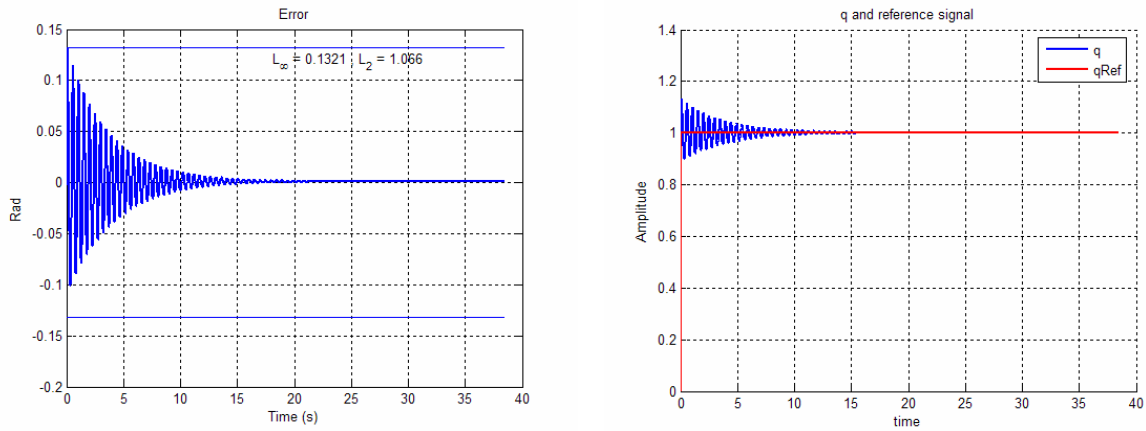


Figure 5. Response and tracking error for $y_{ref} = u(t)$ with initial states [0.05, 0.003, 0.1, 0.1]

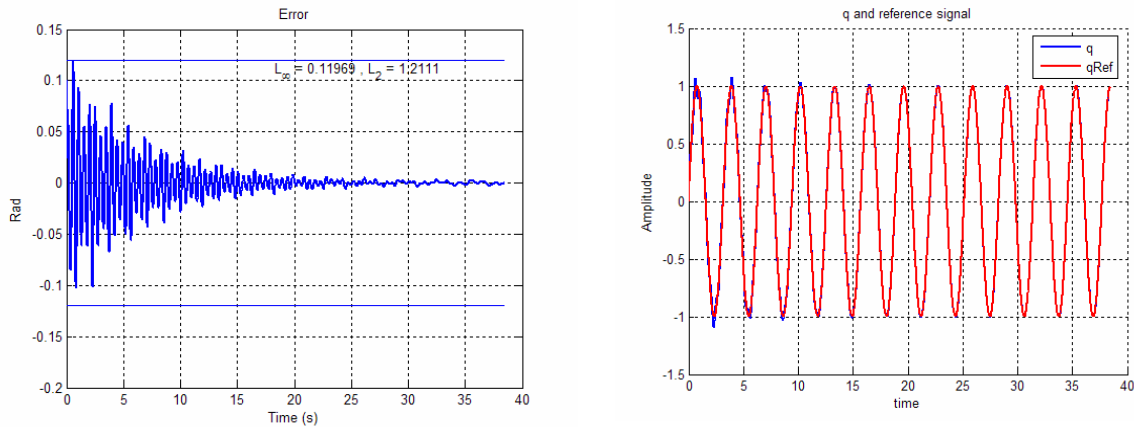


Figure 6. Response and tracking error for $y_{ref} = \sin 2t$ with initial states [0.05, 0.003, 0.1, 0.1]

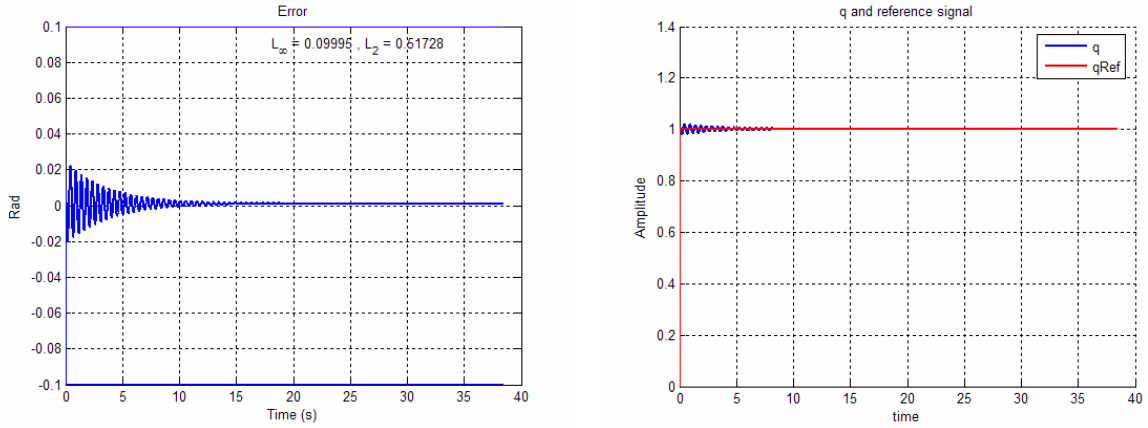


Figure 7. Response and tracking error for $y_{ref} = u(t)$ with zero initial states

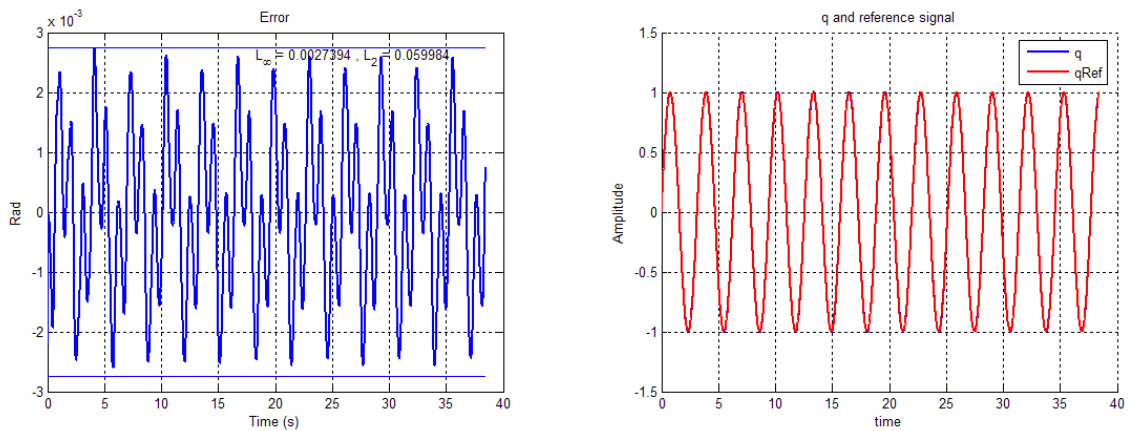


Figure 8. Response and tracking error for $y_{ref} = \sin 2t$ with zero initial states

Table 1. Tracking error comparison over 38.5 s simulation

<i>reference</i>	<i>Initial condition</i>	<i>Error L_2 norm</i>	<i>Error L_∞ norm</i>
$y_{ref} = u(t)$	Non-zero initial states	1.066	0.1321
$y_{ref} = \sin 2t$	Non-zero initial states	1.2111	0.11969
$y_{ref} = u(t)$	Zero initial states	0.51728	0.09995
$y_{ref} = \sin 2t$	Zero initial states	0.059984	0.0027394

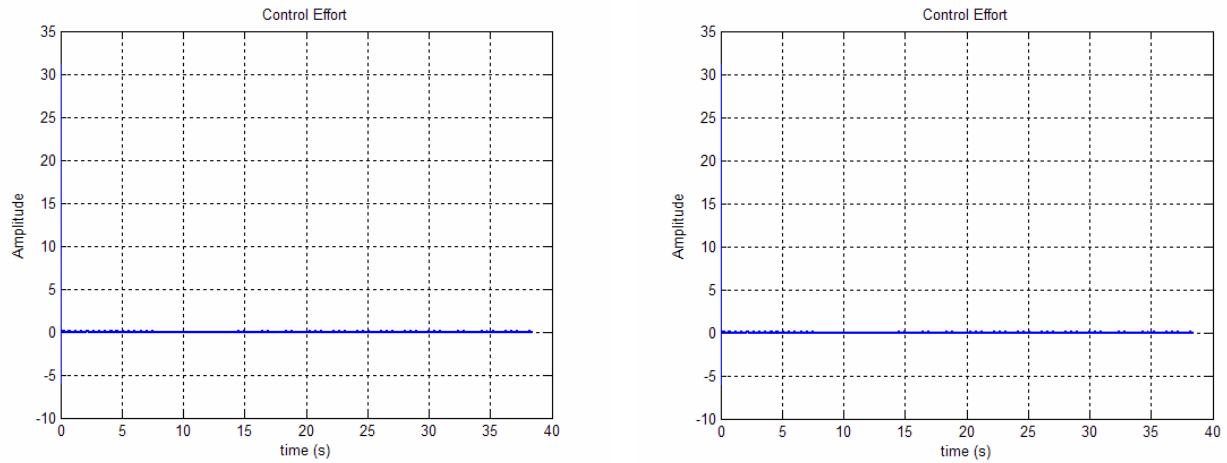


Figure 9. Control effort signal nonzero initial states [0.05, 0.003, 0.1, 0.1] (LEFT) $y_{ref} = u(t)$ (RIGHT) $y_{ref} = \sin 2t$

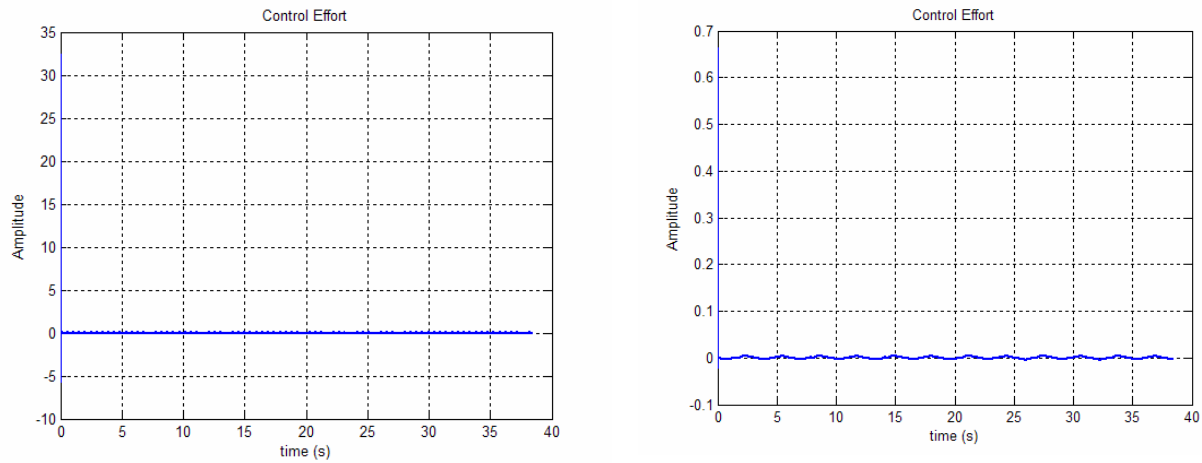


Figure 10. Control effort signal zero initial states (LEFT) $y_{ref} = u(t)$ (RIGHT) $y_{ref} = \sin 2t$

The control signals in Figure 9 and Figure 10 have a large initial value but the reset of the values are completely acceptable. To avoid the large initial values in the control effort, we could smooth the profile of the reference signal to increase slowly at the starting seconds.

As we see in the above table, the error increases as we introduced non-zero initial conditions. The same behavior of error but with lower impacts is when using the *sin* reference instead of $u(t)$. It should be noted that instead of the original $u(t)$, we have used a smoothed version of it to avoid very high frequencies at the reference input, since we are aware of

sensitivity of our design to higher frequencies. The smoothing is carried out by a first order lowpass filter with a far stop-band at $\omega_s = 104.0280$.

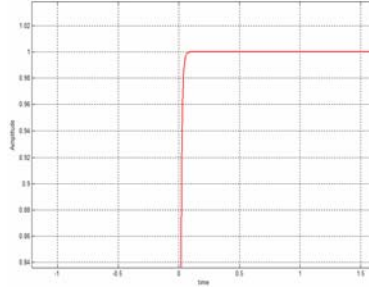


Figure 11. Reference smoothed step function

c. Frequency Analysis

To perform frequency analysis of our design we performed two separate procedures. First, we changed the bandwidth of the closed-loop system by changing the c_1 - c_4 values and observed the error and control effort with $y_{ref} = \sin(2t)$. Second, we set a $y_{ref} = \sin(\omega t)$ and by changing ω we investigate the behavior of error and control signal. In both experiments we used L_2 and L_∞ norms for comparison in fixed simulation times for each. Simulation time of the first set of experiment is set to 150 seconds and the second set is set to 50 seconds. Additionally, we depicted the power spectral density of error and control signal versus the bandwidth.

To analyze the bandwidth of the nonlinear system we used an equivalent measure which could in some sense provide the bandwidth of the system.

We introduce $\frac{\dot{V}}{V} < -\lambda$ and $\lambda > 0$ which in the view of exponential stability ensures that the Lyapunov function decreases exponentially with rate at least equal to λ . In the absence of disturbance and by considering our overall Lyapunov function, we have

$$\frac{\dot{V}}{V} = \frac{-c_1 z_1^2 - \frac{c_2}{2} z_2^2 - \frac{c_3}{2} z_3^2 - \frac{c_4}{2} z_4^2}{\frac{1}{2}(z_1^2 + z_2^2 + z_3^2 + z_4^2)}. \quad \text{Eq. 64}$$

Thus, if we multiply the c_1 - c_4 coefficients by a single gain the convergence rate of the controller to the desired values is increased and therefore the bandwidth of the system is increased. We used 7 different coefficients $\{0.5000, 2.0833, 3.6667, 5.2500, 6.8333, 8.4167, 10\}$ for this purpose and c_1 - c_4 are chosen to be our designed gains in Eq. 61.

It is evident from Figure 12 that by increasing the gain the bandwidth of the controller is increased as well as unwanted higher frequency components of the control effort. The same behavior is observed at the tracking error with some modification due to frequency response of the system. Figure 13 shows the impact of increasing bandwidth on the tracking error and control signal norms when the reference signal is kept at $y_{ref} = \sin(2t)$. As it could be already expected increasing the bandwidth increases the tracking error as well as the control effort.

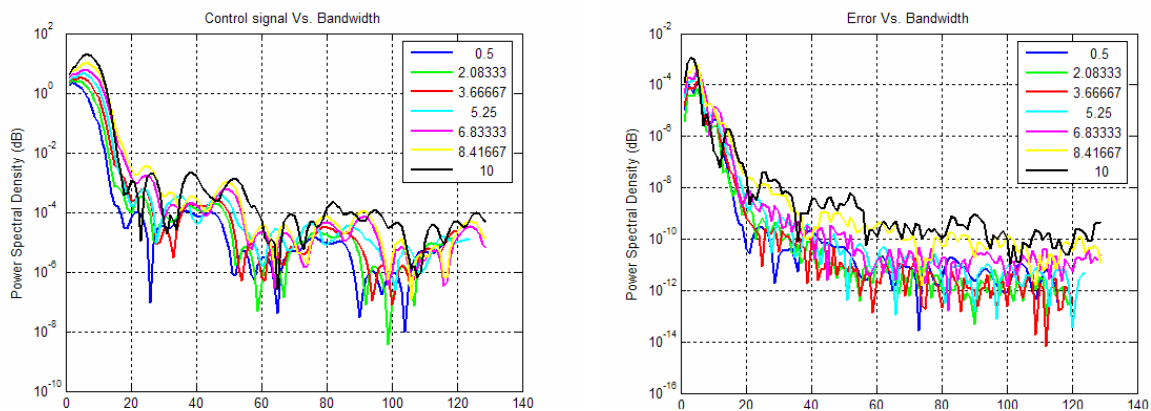


Figure 12. Power spectral density variation due to changes in bandwidth. (Left) Control signal (Right) Error

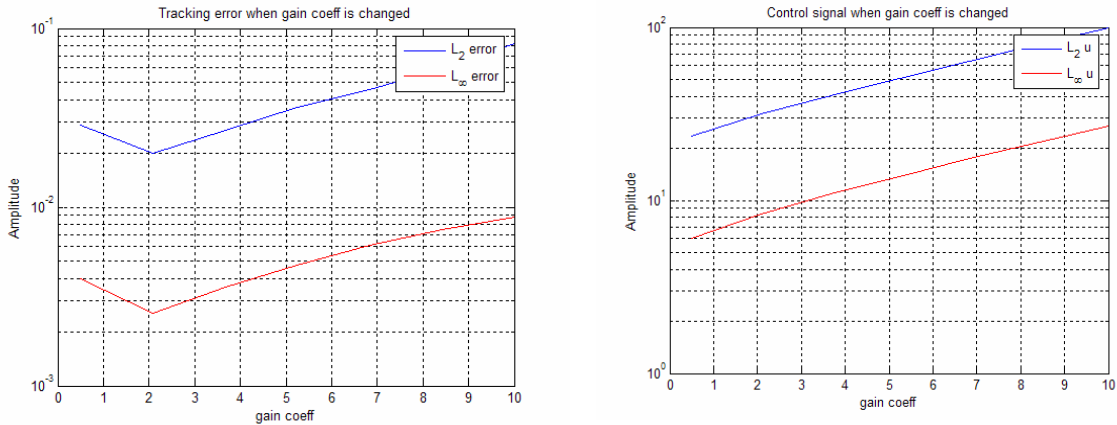


Figure 13. Impact of changing the bandwidth on (Left) Tracking error (Right) control signal

To analyze the frequency response of the closed-loop system, we introduced reference signal as $y_{ref} = \sin(\omega t)$ with $\omega = \{1, 5, 10, 15, 20, 25, 30, 35, 40\}$ and observed the same values of the system. Almost similar results have obtained from this experiment as the previous. Figure 14 represents that the close-loop bandwidth is far more than $\omega_b = 2$ and the performance of the controller deteriorates with increase in reference frequency. This behavior is accompanied by increase in control effort which is a quite usual phenomenon.

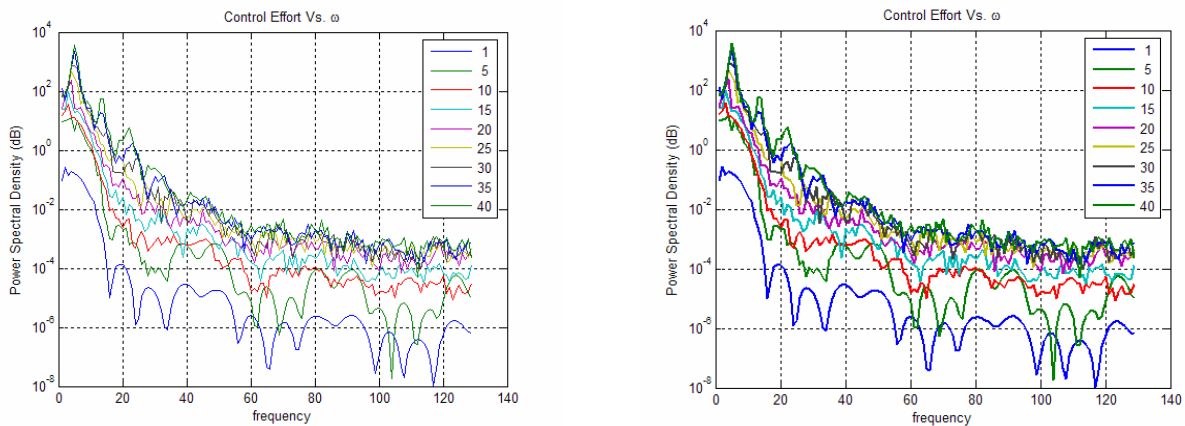


Figure 14. Power spectral density variation due to change in frequency of reference signal (Left) Control Signal (Right) Error

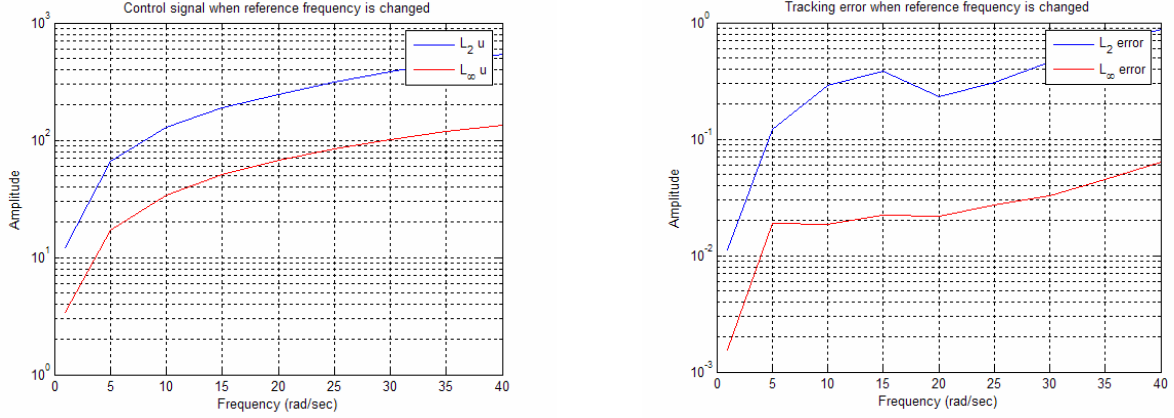


Figure 15. Impact of changing the frequency of reference signal on (Left) Tracking error (Right) control signal

d. Parameter Uncertainty

As we mentioned in the earlier discussion, backstepping design provides means to build a robust controller which could handle parameter uncertainties as well as disturbances. In the dimensionless equations of Eq. 26 and Eq. 27 the input signal and disturbance signal are scaled with nominal parameter values. If the parameters change from their nominal values the supposed model will not be valid anymore and the input control signal and disturbance signal should be multiplied by some values imposed by new parameters.

Relation between input and disturbance signal (N and F) on the main system and the dimensionless equation is as

$$\left\{ \begin{array}{l} \xi = \sqrt{\frac{M+m}{I+me^2}} q \\ \varepsilon = \frac{me}{\sqrt{(I+me^2)(M+m)}} \\ u = \frac{(M+m)}{k(I+me^2)} N \\ \tau = \sqrt{\frac{k}{M+m}} t \\ w = \frac{1}{k} \sqrt{\frac{M+m}{I+me^2}} F \end{array} \right. \quad \text{Eq. 65}$$

Thus, we should be aware that changing in parameters changes the gains of u and w as well as τ . Relations in Eq. 65 suggests that if we calculate the bound of ε , coefficients that transforms t to τ , F to w , and N to u and test the designed controller for the system parameters (K , I , m , M) that produced these bounds the robustness of the closed-loop system to the parameter changes is examined. Hence, we used a computer program to calculate the bounds of these variables as the parameters change in their bound. The results in Table 2 show the bound of variables and their nominal values.

Table 2. Bound of parameter uncertainty and the corresponding values of parameters for system in Eq. 26 and Eq. 27.

Case	Variable	Type	Value	K	I	m	M
	ε	Nominal	0.2118	187.86	2.2e-3	0.09	1.1
1.	ε	min	0.2651	184.14	2.17e-3	0.11	0.9
2.	ε	max	0.2375	186	22e-4	0.1	1
	$\tau \rightarrow t$ coefficient	Nominal	12.3362	184.14	-	0.11	1.1
3.	$\tau \rightarrow t$ coefficient	Min	13.7753	187.86	-	0.09	1.1
4.	$\tau \rightarrow t$ coefficient	Max	13	186	-	0.1	1
	$u \rightarrow N$ coefficient	Nominal	8.6968	187.86	22e-4	0.11	0.9
5.	$u \rightarrow N$ coefficient	min	11.92	184.14	2.17e-3	0.09	1.1
6.	$u \rightarrow N$ coefficient	max	10.2	186	22e-4	0.1	1
	$w \rightarrow F$ coefficient	Nominal	0.2152	184.14	2.17e-3	0.11	1.1
7.	$w \rightarrow F$ coefficient	min	0.2145	184.14	2.17e-3	0.09	1.1
8.	$w \rightarrow F$ coefficient	max	0.2341	186	22e-4	0.1	1

Now we are ready to simulate the system with these parameter uncertainties. in the above table, there are 8 cases which 5 of them are unique (case 5 and 6 are equal to 7 and 8 respectively and case 6 is the same as case 2). We have simulated the system with backstepping controller with these 5 different cases of parameters and as the results in Figure 16 to **Error! Reference source not found.** shows our controller has the ability to handle parameter uncertainty with the in the specified bound.

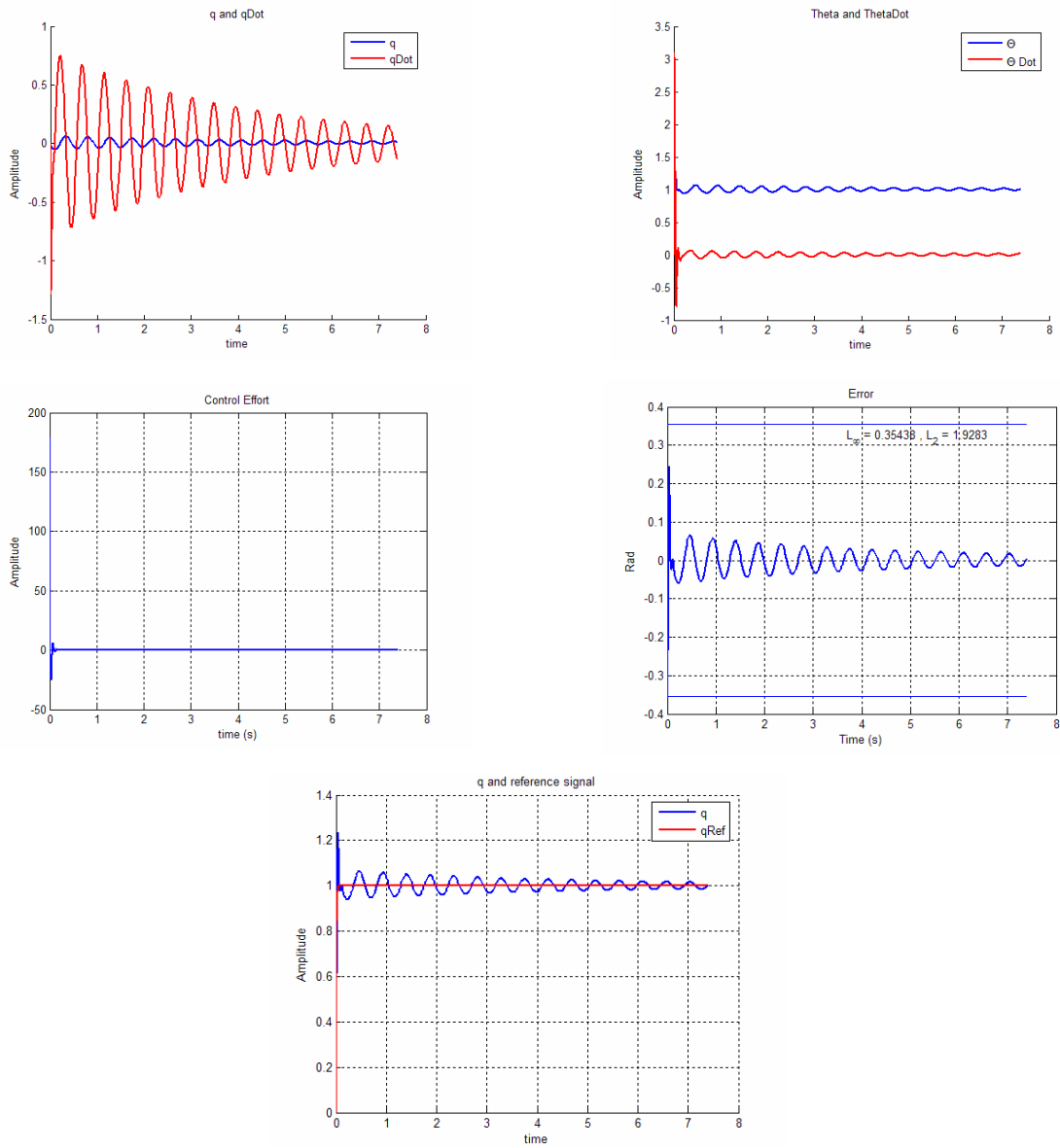


Figure 16. Case 1 of Table 2 (Top-Left) q and \dot{q} (Top-Right) θ and $\dot{\theta}$ (Middle-Left) Control Effort (Middle-Right) Tracking Error (Bottom) q and reference signal

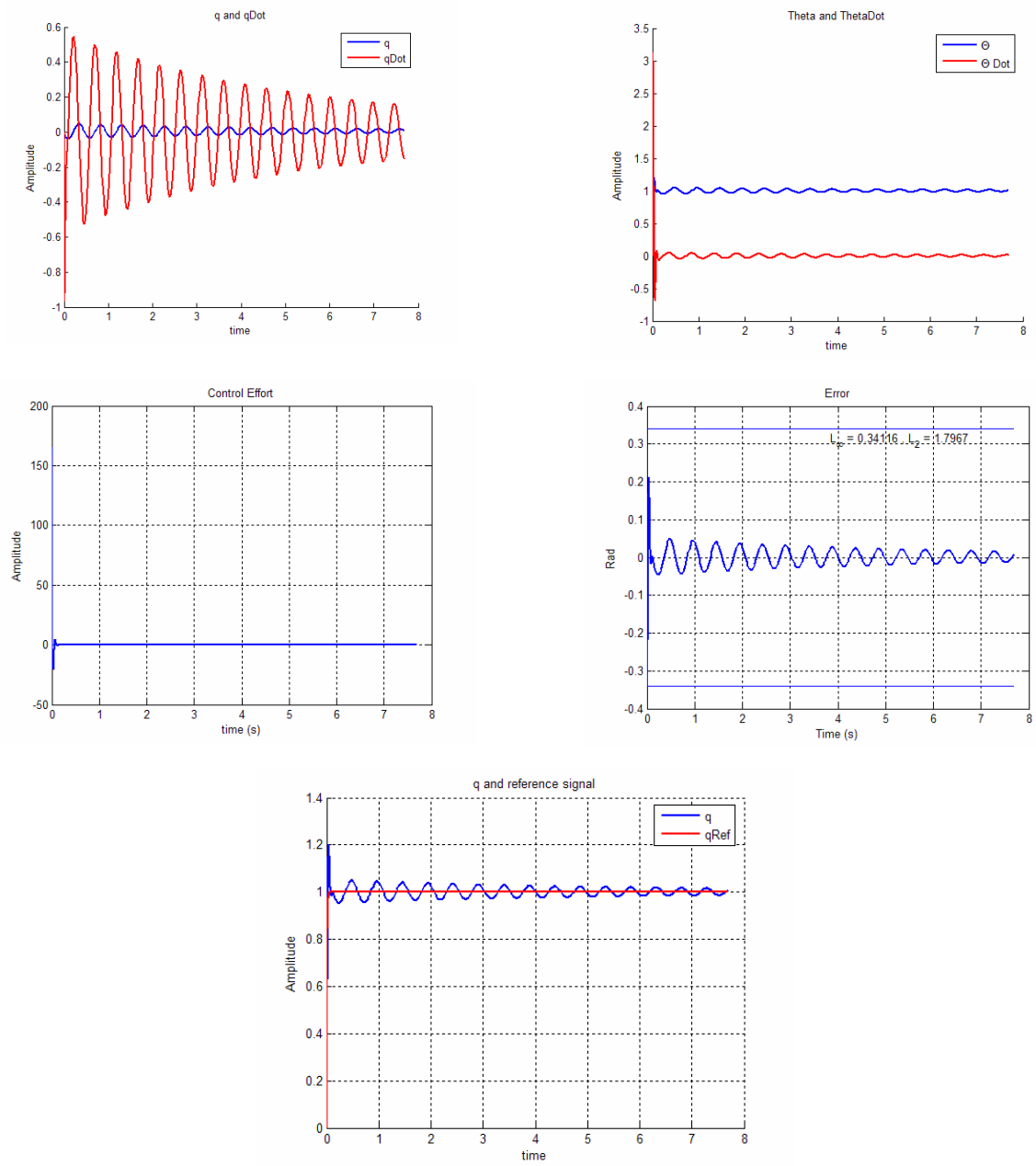


Figure 17. Case 2 of Table 2 (Top-Left) q and \dot{q} (Top-Right) θ and $\dot{\theta}$ (Middle-Left) Control Effort (Middle-Right) Tracking Error (Bottom) q and reference signal

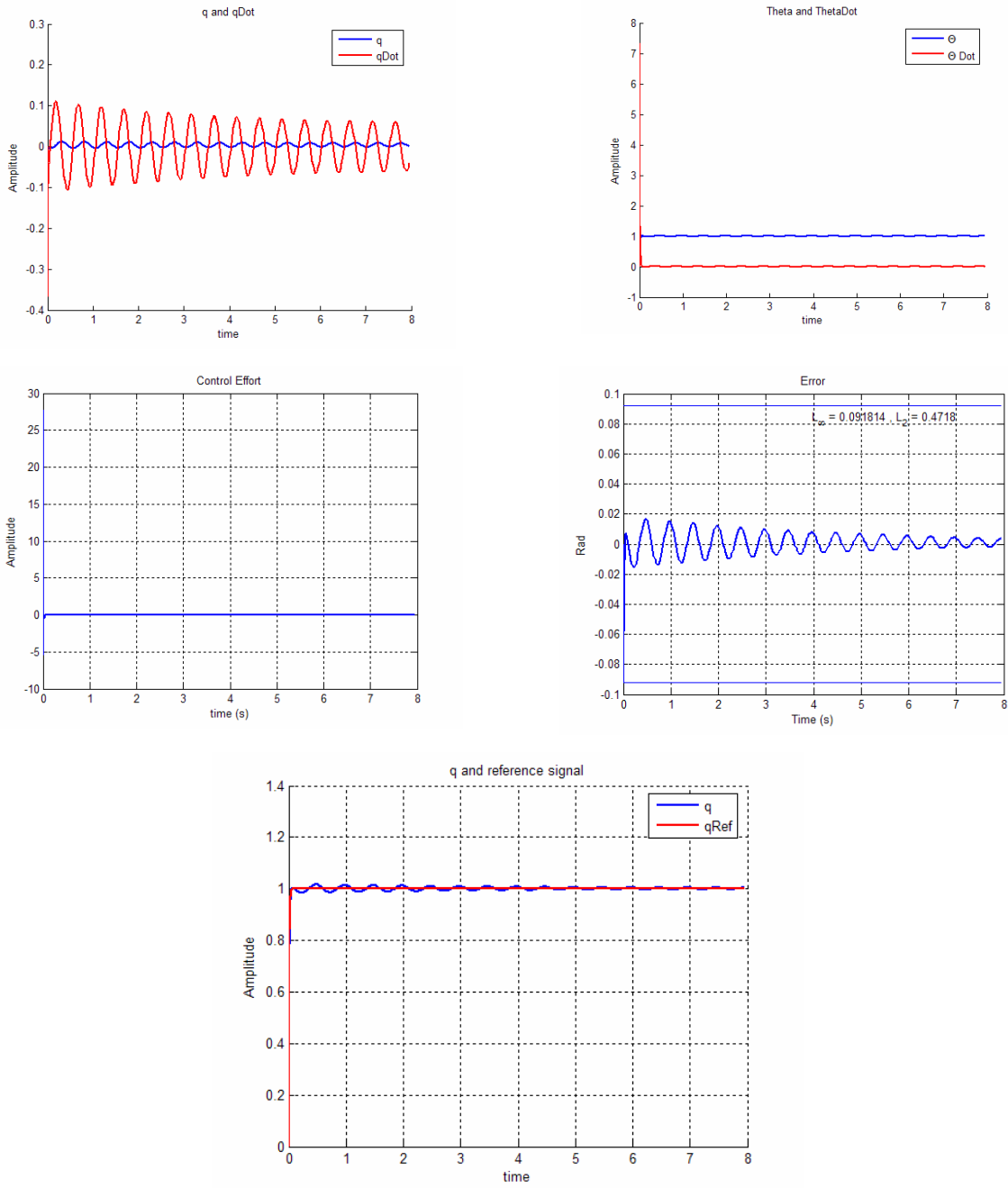


Figure 18. Case 3 of Table 2 (Top-Left) q and \dot{q} (Top-Right) θ and $\dot{\theta}$ (Middle-Left) Control Effort (Middle-Right) Tracking Error (Bottom) q and reference signal

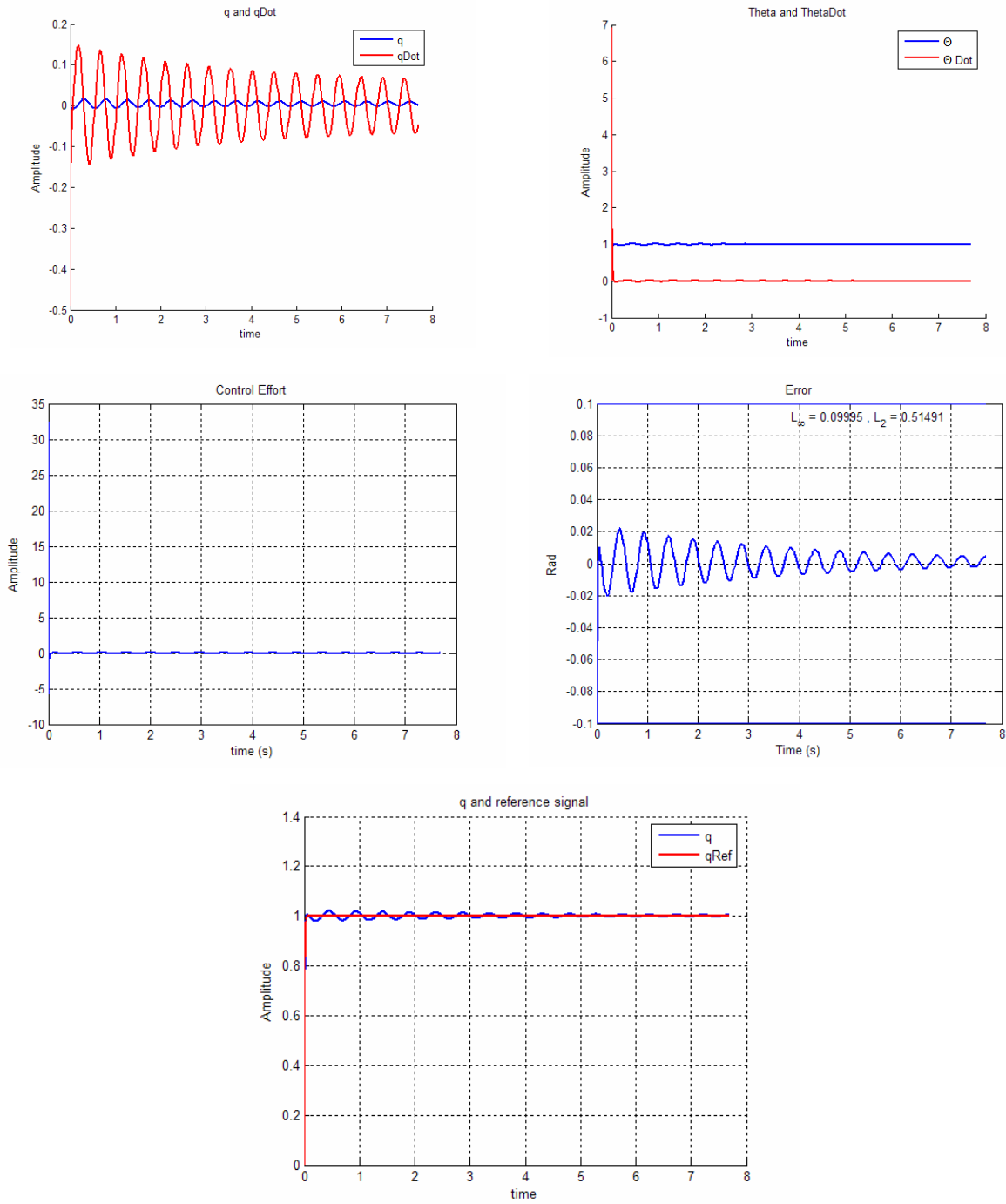


Figure 19. Case 4 of Table 2 (Top-Left) q and \dot{q} (Top-Right) θ and $\dot{\theta}$ (Middle-Left) Control Effort (Middle-Right) Tracking Error (Bottom) q and reference signal

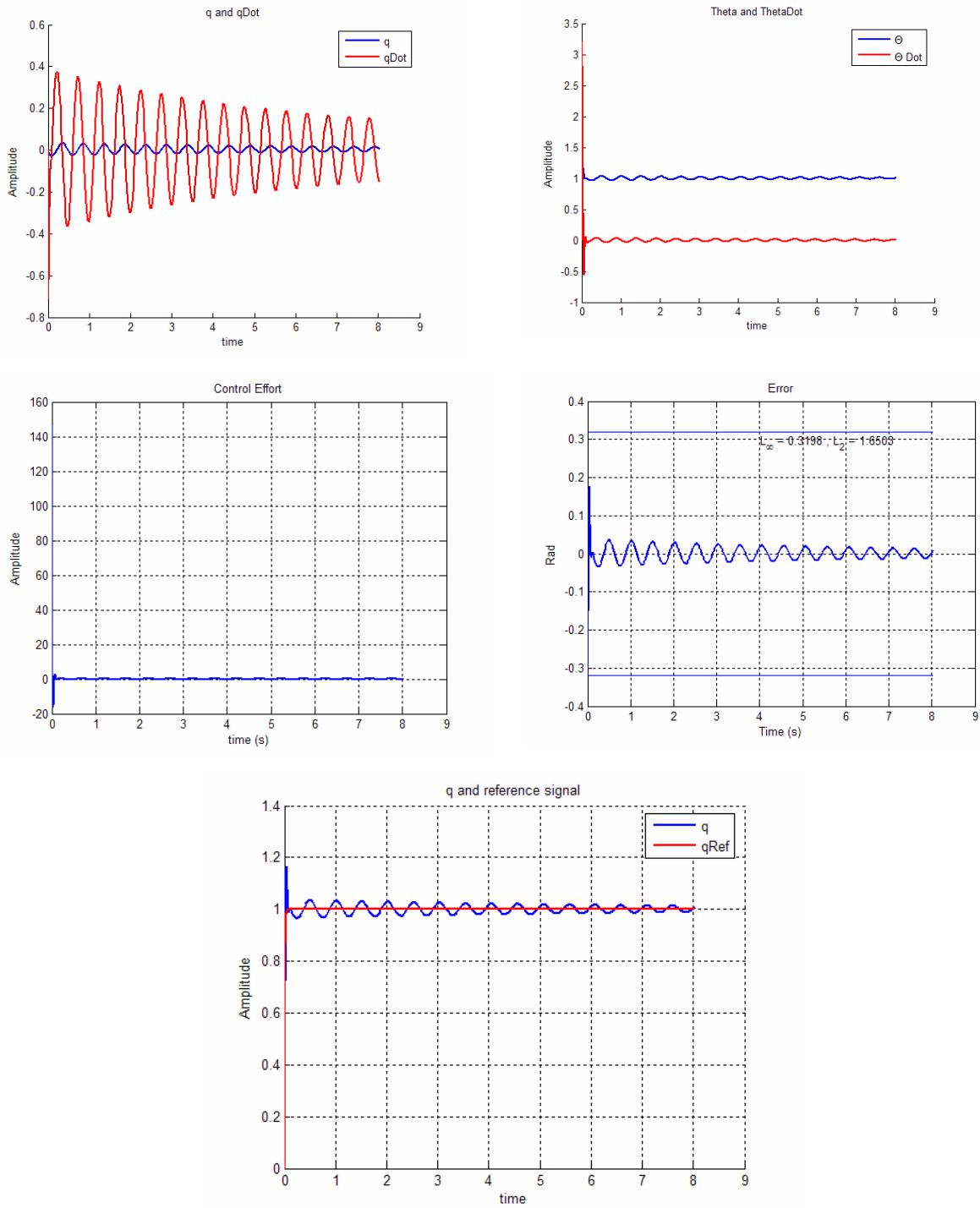


Figure 20. Case 5 of Table 2 (Top-Left) q and \dot{q} (Top-Right) θ and $\dot{\theta}$ (Middle-Left) Control Effort (Middle-Right) Tracking Error (Bottom) q and reference signal

To sum up our results in this section, we introduce the table below which compares the error of different parameter uncertainty cases with the nominal system. Table 3 shows that our controller is more sensitive to the first case of uncertainties, which as it could be expected is ε .

Table 3. Tracking error of different cases of parameter uncertainty

<i>Uncertainty Case</i>	<i>Tracking Error L_2 Norm</i>
1.	1.92
2.	1.79
3.	0.4718
4.	0.51
5.	1.65

e. Disturbance Attenuation

To show the ability of our controller in disturbance attenuation we will use the same configuration as in **Error! Reference source not found.** for disturbance were $F(t) = 8 \sin(t)$ and we will calculate $E(t) = \dot{\theta}^2 + \dot{\xi}^2 + \xi^2 - mgr \cos(\theta)$ as a function of physical energy of the system and we show that this function will be bounded and since it is a monotonically increasing function of system physical energy (a convex function), we could conclude that the physical system is stable in Lyapunov sense. This behavior is depicted in Figure 21 and Figure 22 shows the effect of such a disturbance on the performance and behavior of the system.

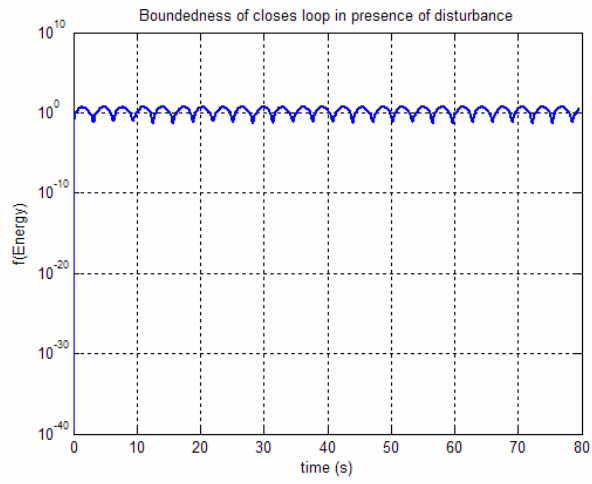


Figure 21. Function of physical energy of the system $E(t) = \dot{\theta}^2 + \dot{\xi}^2 + \xi^2 - mgr \cos(\theta)$

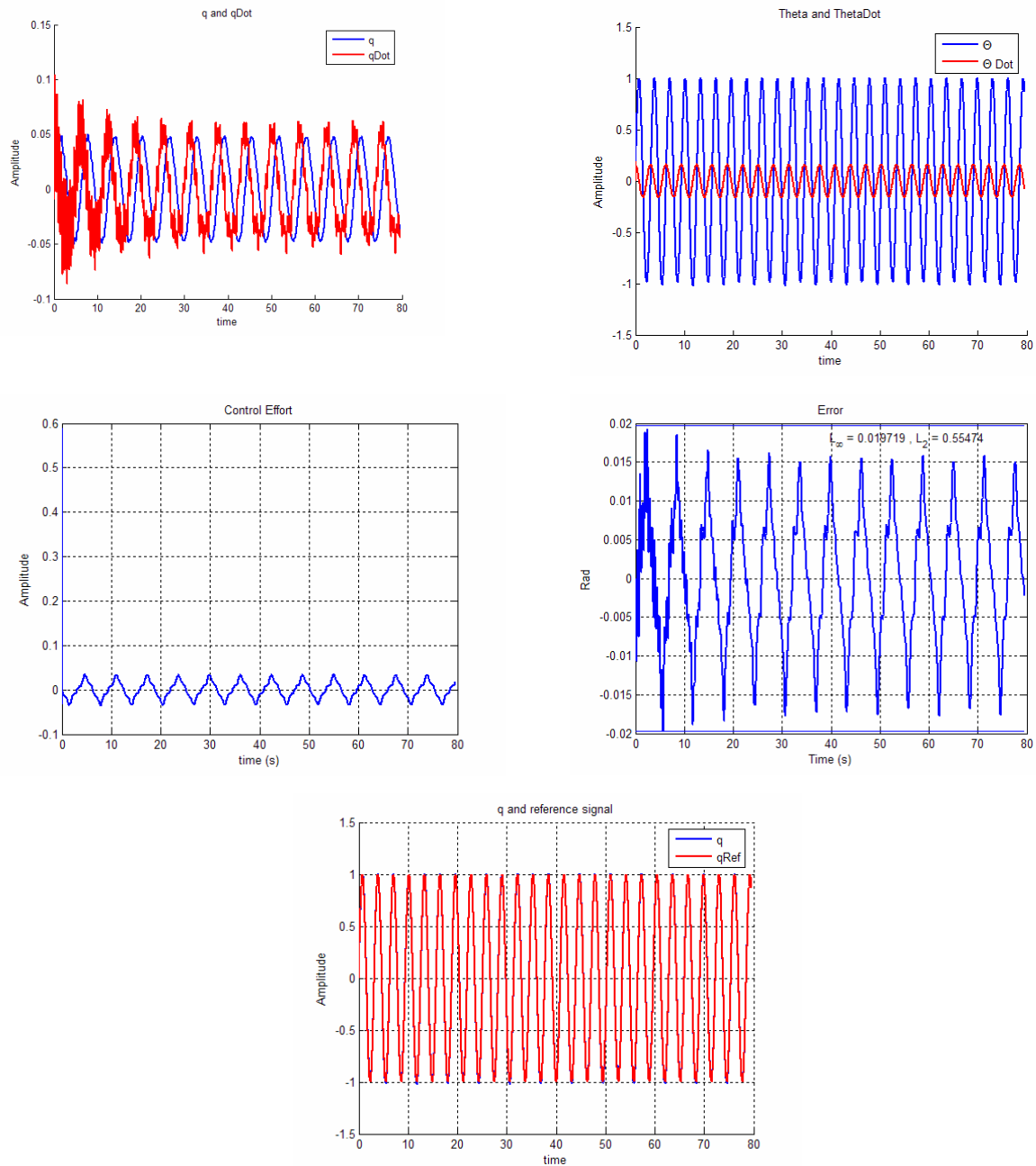


Figure 22. Disturbance attenuation with $F(t) = \sin(t)$ and $y_{ref} = \sin(2t)$ (Top-Left) q and \dot{q} (Top-Right) θ and $\dot{\theta}$ (Middle-Left) Control Effort (Middle-Right) Tracking Error (Bottom) q and reference signal

3-3 Saturation of actuator

In this section, we add a saturation of actuator with ± 1 saturation limit to the system and observe the result. Naturally, we anticipate increase of oscillation and in sever cases it will lead to instability but in this case it just increases the oscillation (Figure 23).

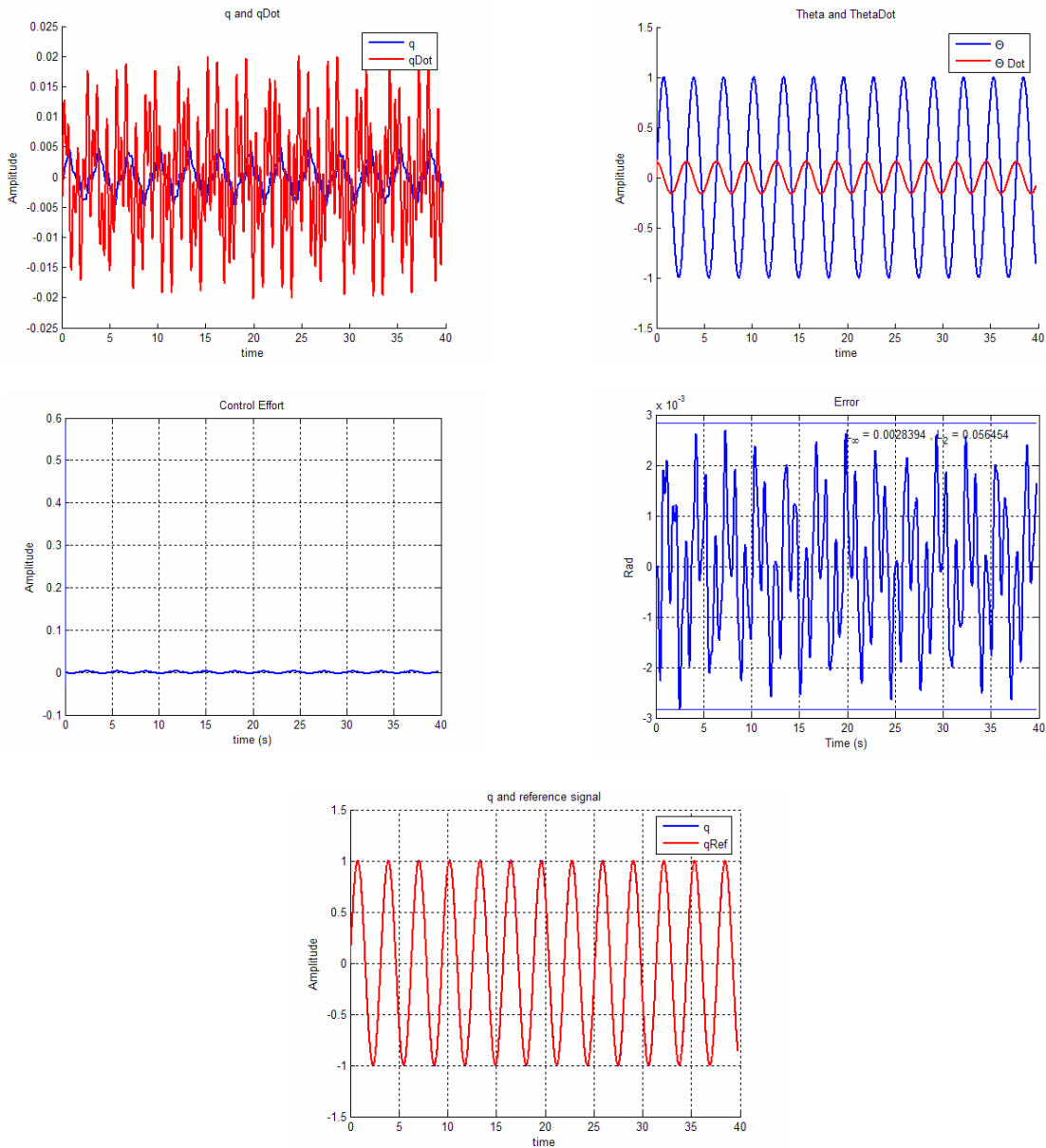


Figure 23. Effect of saturation of actuator with ± 1 limit (Top-Left) q and \dot{q} (Top-Right) θ and $\dot{\theta}$ (Middle-Left) Control Effort (Middle-Right) Tracking Error (Bottom) q and reference signal

Now we investigate the minimum saturation level that deteriorates the tracking. Figure 24 show the increase of tracking error as saturation level decreases. Considering the results in this figure, we conclude that minimum acceptable saturation level for this controller ± 0.2 .

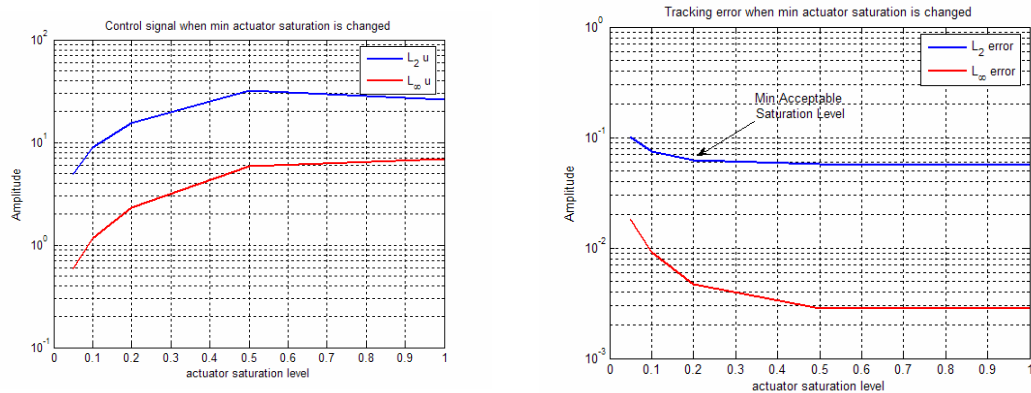


Figure 24. Effects of changing actuator saturation level on tracking
(Left) Norms of Control signal (Right) Norms of tracking error

3-4 Sliding Mode Controller

a. Brief Review

Model imprecision may come from actual uncertainty about the plant, or from the purposeful choice of a simplified representation of system's dynamics. From a control point of view, modeling inaccuracies can be classified into two major kinds:

- Structured uncertainties
- Unstructured uncertainties

The first kind corresponds to inaccuracies on the terms actually included in the model, while the second kind corresponds to inaccuracies on the system's order [8]. The main idea of sliding mode control is to transform the original tracking control problem into a simple *first-order* stabilizing problem. Namely, the intuitive feedback control rule which says: "if the

error is negative, push hard enough in the positive direction" actually works for first-order system and it does not work for higher-order systems. In addition, sliding mode provides a systematic approach to the problem of maintaining stability and consistent performance in the face of modeling imprecision.

b. Controller Design

Considering sliding mode design, we should convert the state equations into the form of

$$\dot{x}^{(n)} = f(x) + b(x)u \quad \text{Eq. 66}$$

We use Eq. 1 and Eq. 2 and by letting $F=0$ we derive

$$\ddot{\theta} = \frac{me \dot{\theta}^2 \sin \theta}{me \cos \theta - \frac{I + me^2}{\varepsilon \cos \theta}} - \frac{k}{me \cos \theta - \frac{I + me^2}{\varepsilon \cos \theta}} q - \frac{\frac{N}{\varepsilon \cos \theta}}{me \cos \theta - \frac{I + me^2}{\varepsilon \cos \theta}}$$

and finally,

$$\ddot{\theta} = \frac{me \varepsilon \dot{\theta}^2 \sin 2\theta}{2(m\varepsilon \cos^2 \theta - I - me^2)} - \frac{k\varepsilon \cos \theta}{m\varepsilon \cos^2 \theta - I - me^2} q - \frac{N\varepsilon}{m\varepsilon \cos^2 \theta - I - me^2}$$

Thus, we have

$$f(\theta, \dot{\theta}) = \frac{me \varepsilon \dot{\theta}^2 \sin 2\theta}{2(m\varepsilon \cos^2 \theta - I - me^2)} - \frac{k\varepsilon \cos \theta}{m\varepsilon \cos^2 \theta - I - me^2} q \quad \text{Eq. 67}$$

$$b = -\frac{\varepsilon}{m\varepsilon \cos^2 \theta - I - me^2}$$

which represents the system in the form of Eq. 66. If you consider the term which includes q as the unstructured uncertainties we could have a simpler equation as

$$\hat{f}(\theta, \dot{\theta}) = \frac{me \varepsilon \dot{\theta}^2 \sin 2\theta}{2(m\varepsilon \cos^2 \theta - I - me^2)}.$$

Besides, we tend to consider the parameter uncertainties and this leads us to write

$$\hat{f} = \frac{f_{\max} + f_{\min}}{2}$$

Where

$$f_{\max} = b_{\max} \left[k_{\max} \frac{m_{\max}}{M_{\max} + m_{\max}} \times (q + \varepsilon_{\max}) + m_{\max} \varepsilon_{\max} e \right]$$

$$f_{\min} = b_{\min} \left[k_{\min} \frac{m_{\min}}{M_{\max} + m_{\max}} \times (q - \varepsilon_{\max}) + m_{\min} \varepsilon_{\max} e \right]$$

With

$$b_{\min} = \frac{\varepsilon_{\min}}{I_{\max} + m_{\max} e^2 - m_{\max} e m_{\max} \frac{e}{M_{\min} + m_{\min}}}, \varepsilon_{\max} = \frac{m_{\max} e}{M_{\min} + m_{\min}}, \varepsilon_{\min} = \frac{m_{\min} e}{M_{\max} + m_{\max}}$$

$$b_{\max} = \frac{\varepsilon_{\max}}{I_{\min} + m_{\min} e^2 - m_{\max} e m_{\max} \frac{e}{M_{\min} + m_{\min}}}$$

We introduce tracking error as $e = x - x_d$ and we begin with the procedure of designing a sliding mode controller with

$$s = \left(\frac{d}{dt} + \lambda \right) e = \dot{e} + \lambda e \rightarrow \dot{s} = \ddot{e} + \lambda \dot{e} = \ddot{x} - \ddot{x}_d + \lambda \dot{e} = f + bu - \ddot{x}_d + \lambda \dot{e} \quad \text{Eq. 68}$$

We introduce the sliding mode Lyapunov function $V = \frac{1}{2} s^2$ and we intend to have the control law which outside of the surface $s=0$ has the sliding condition which is

$$\frac{1}{2} \frac{d}{dt} s^2 \leq -\eta |s| \quad \text{Eq. 69}$$

This leads us to a controller that asymptotically moves toward the sliding surface and when it reaches there it should be stay on the surface.

Thus, $\dot{s} = 0$ gives us the control law

$$u = [-f + \ddot{x}_d - \lambda \dot{e}] \quad \text{Eq. 70}$$

But as we have simplified equations which have unstructured and parameter uncertainties we introduce a equivalent control as

$$\hat{u} = [-\hat{f} + \ddot{x}_d - \lambda \dot{e}] \quad \text{Eq. 71}$$

Now, in order to satisfy sliding condition despite uncertainty on the dynamics f , we add to \hat{u} a term discontinuous across the surface $s=0$

$$u = \frac{1}{\hat{b}}(\hat{u} - k \operatorname{sgn}(s)) \quad \text{Eq. 72}$$

where $\hat{b} = \sqrt{b_{\min} b_{\max}}$.

In this project, we are assumed to design two sliding controllers, one with hard switch and another with a soft switching. Thus, we introduce

$$u = \left(\frac{1}{\hat{b}}\right) \times \left[-\hat{f} + \ddot{x}_d - \lambda \dot{e}\right] + \left(\frac{1}{\hat{b}}\right) \times k \operatorname{sign}(s) \quad \text{Eq. 73}$$

for hard switching and

$$u = \left(\frac{1}{\hat{b}}\right) \times \left[-\hat{f} + \ddot{x}_d - \lambda \dot{e}\right] + \left(\frac{1}{\hat{b}}\right) \times \frac{k}{\Phi} \operatorname{sat}(s) \quad \text{Eq. 74}$$

for soft swathing, where Φ is the slope of the soft switch. The soft switch decreases the chattering effect in trade-off with increase in tracking error.

The above procedure or sliding mode controller design indicates that the designer have many different parameters to tune for his/her needs in this method. First, η sets the convergence rate to the sliding surface when the system is out of $S(t)$. The second parameter is λ which indicates the closed-loop bandwidth of the sliding controller and specifies the speed of convergence to the desired values when state variables are on the sliding surface. Finally, Φ specifies the slope of the soft switch and could be used to decrease chattering and increase the closed-loop bandwidth.

3-5 Implementation

For a typical design, we consider $k=20$, $\lambda=10$ and $\eta=0.1$ with sign function as the switch and $y=\theta$ as the output. First, the desired output is unit step function.

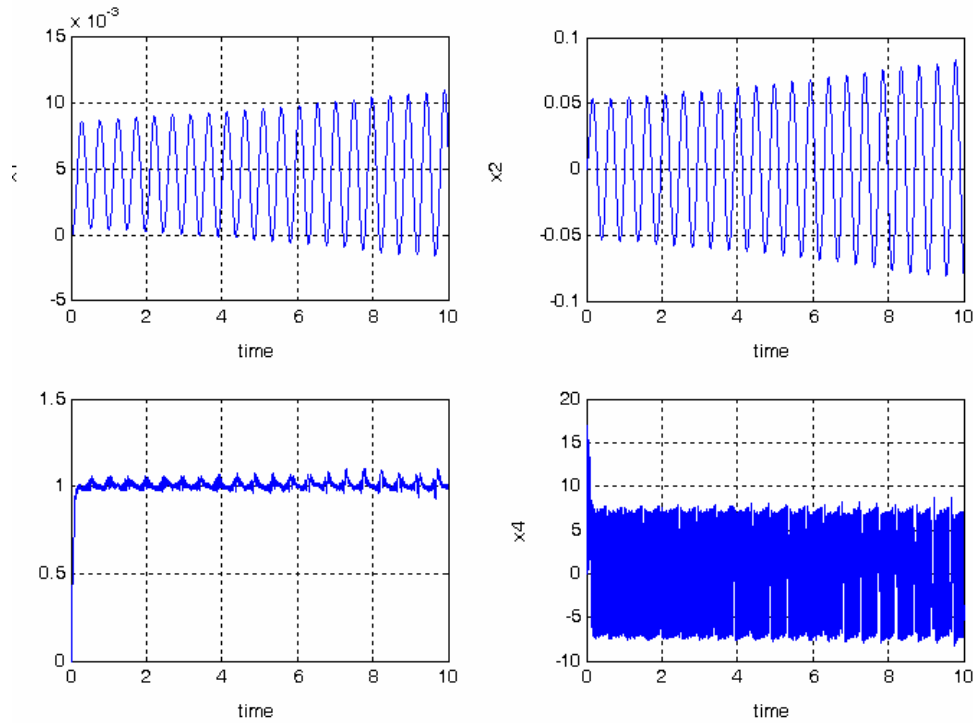


Figure 25. State variables $k=20$, $\lambda = 10$, $\eta = 0.1$, $y_{ref}=u(t)$

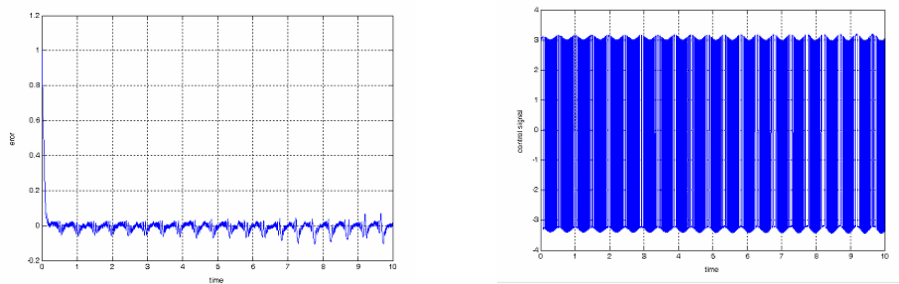


Figure 26. (Left) Tracking Error (Right) Control effort

The important point to notice is that the control signal has very large high frequency components which lead to chattering in output state. These large frequency components will invoke un-modeled dynamics of the system more and creates more error.

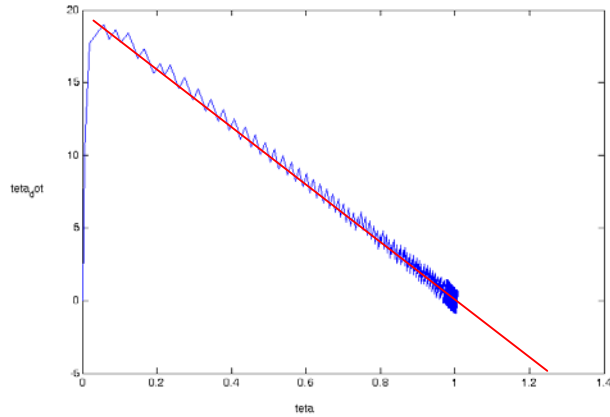


Figure 27. Phase plane of the simple sliding mode controller

Figure 27 shows the sliding mode action with a first the capture and then surfing behavior of the state variables on the sliding surface.

Now, we investigate the ability of our controller to track $y_{ref} = \sin(2t)$ with the same control parameters.

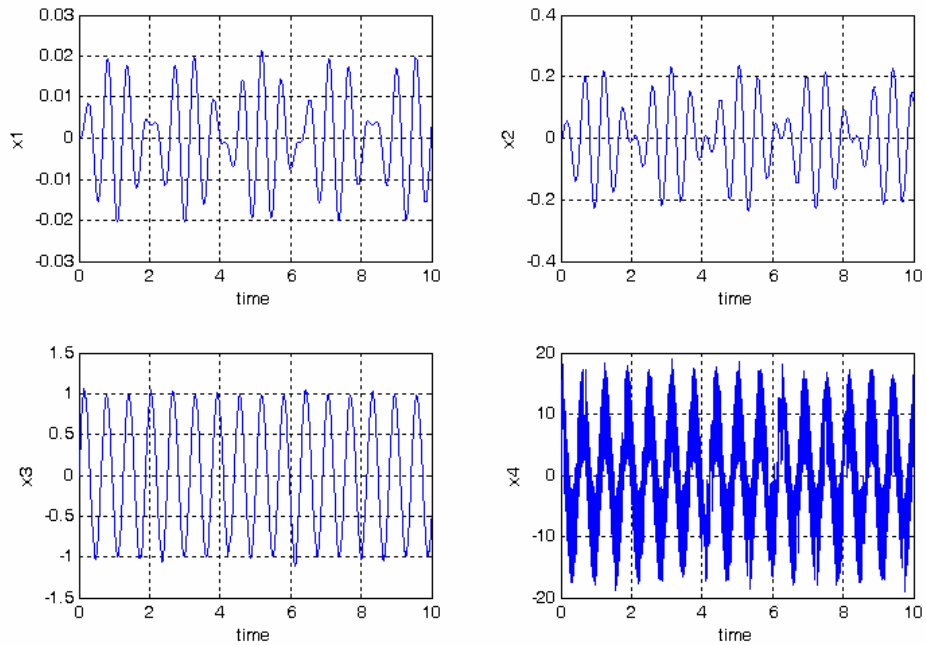


Figure 28. State variables $k=20$, $\lambda = 10$, $\eta = 0.1$, $y_{ref} = \sin(2t)$

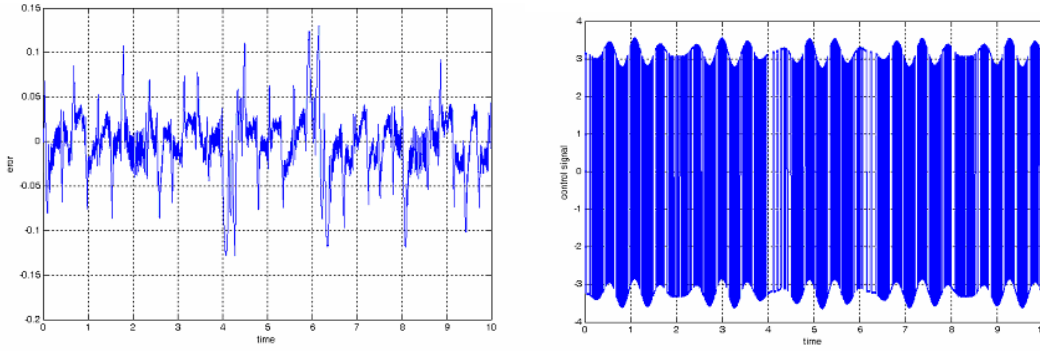


Figure 29. (Left) Tracking Error (Right) Control effort

The same high frequency behavior is observed here for a different reference input. In fact, the high frequency is created by the fast switching between to large positive and negative values in u . From these results, it is evident that this control effort is completely undesirable and we should design a soft switch to avoid this behavior.

a. Bandwidth Analysis

In sliding mode controller, we have explicit measure of closed-loop bandwidth which is value of λ and this contradicts with backstepping which does not have explicit definition of bandwidth. Intuitively, we expect that increasing λ will increase the speed of the system and decreases the tracking error on the sliding surface. Figure 30 shows the result of changing λ on tracking error and control signal. From Figure 30 it is evident that is fast convergence comes with trade-off with higher control effort.

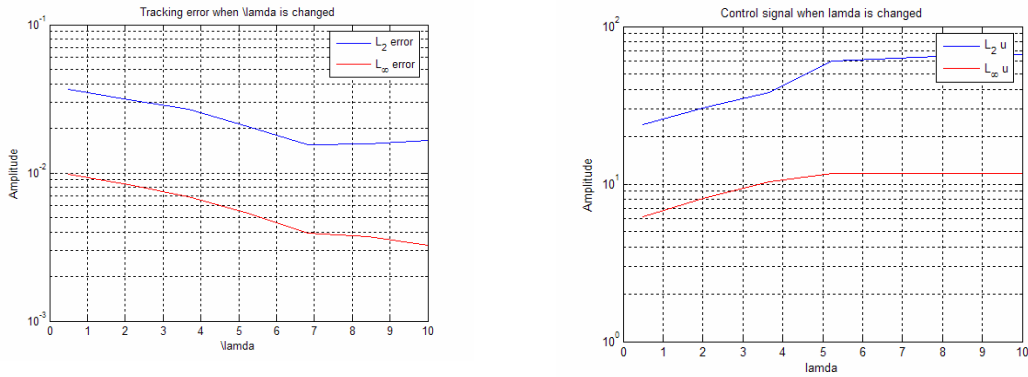


Figure 30. Bandwidth effect (Left) Tracking Error (Right) Control effort

b. Analysis Different

We anticipate that increasing the value of k , which is a upper measure of uncertainties outside the sliding surface, will increase the chattering and control effort as well.

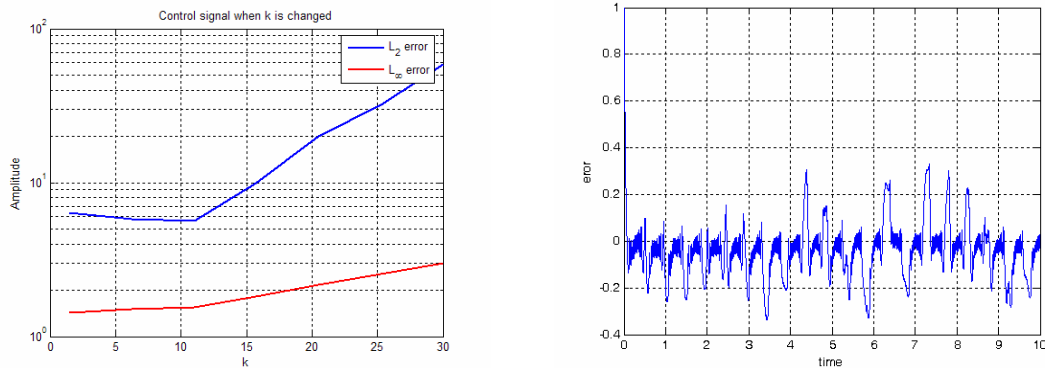


Figure 31. Effects of changing k (Left) Control signal (Right) Tracking error at $k=30$ $y_{ref}=u(t)$
 Figure 31 shows the sharp increase in control signal as k increases and the large tracking error due to rapid chattering at $k = 30$.

c. Actuator Saturation

The level of saturation of the actuator has direct impact on the behavior of the system and imposes a very practical constraint on the controller design. As we are experience in backstepping with saturation level, we expect here to see increase of oscillation with presence of saturation. We examine this for $k = 10$, $\lambda = 20$ and saturation levels at $\{1, 1.5, 2\}$ when $y_{ref}=u(t)$. Since all these saturation levels are far below the needed control

effort in Figure 26, the tracking error does not change significantly. However, the interesting result is that sliding mode controller with hard switching method need an actuator with higher level of saturation is expensive.

Table 4. Effect of actuator saturation on sliding mode tracking error

<i>Saturation Level</i>	<i>Tracking Error L2 Norm</i>
1	5.6e-2
1.5	5.3e-2
2	5.1e-2

d. Robustness to Parameter Uncertainties

Sliding mode is intrinsically a robust controller and we expect it to behave so. We have tested the system performance under parameter uncertainty which was introduced in Figure 3, but unfortunately we had no time to prepare the results for this report.

3-6 Soft Switching

In the last section we have designed a controller which is able to handle parameter uncertainties. However, it is not very robust to the dynamical uncertainties. In fact, the controller we designed in the last section does not guarantee that the states $[q, \dot{q}]$ maintain boundedness. Therefore, we should consider a method to handle these uncertainties.

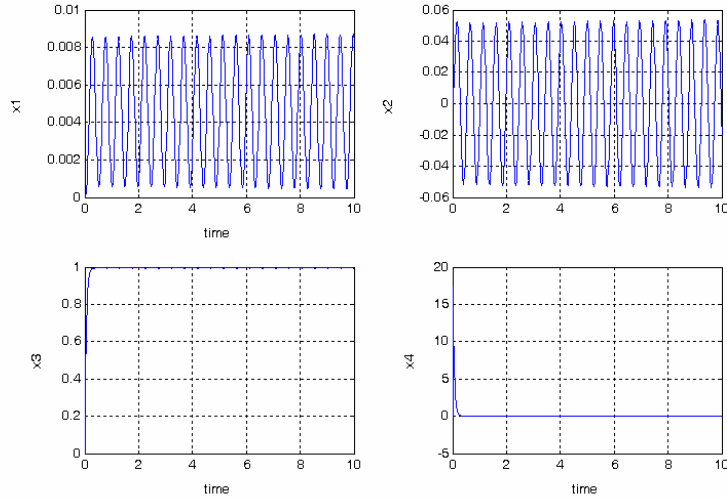


Figure 32. State variables with soft switching sliding mode $\Phi = 10$, $k = 5$, $\lambda = 2$ و $y_{ref}=u(t)$

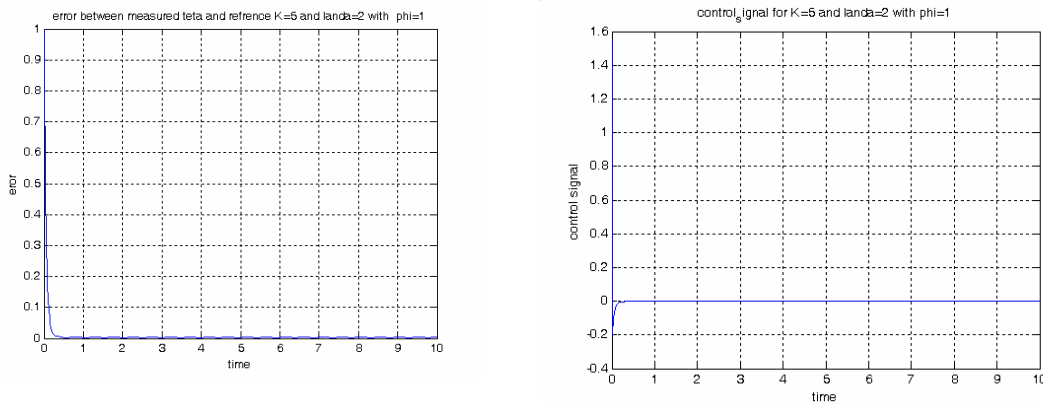


Figure 33. soft switching sliding mode $\Phi = 10$, $k = 5$, $\lambda = 2$, $y_{ref}=u(t)$
 (Left) Tracking Error (Right) Control Signal

A time varying soft switching method is mean to resolve this. This means that we should dynamically calculate the bounds of uncertainty and assign proper Φ in Eq. 74. Meanwhile, Φ have balancing property which compromises between chattering and performance.

Table 5. Φ Balance condition

Φ	Tracking Error	Chattering	Bandwidth
↑	↑	↓	↓
↓	↓	↑	↑

However, we create a simpler dynamics for Φ which make it large at the starting moments and decreases almost exponentially to a fixed value. This behavior improves the handling of unstructured uncertainties as well as improves the tracking performance as time elapses. Figure 34 shows the profile of Φ versus time. The elimination of chattering is depicted in Figure 37.

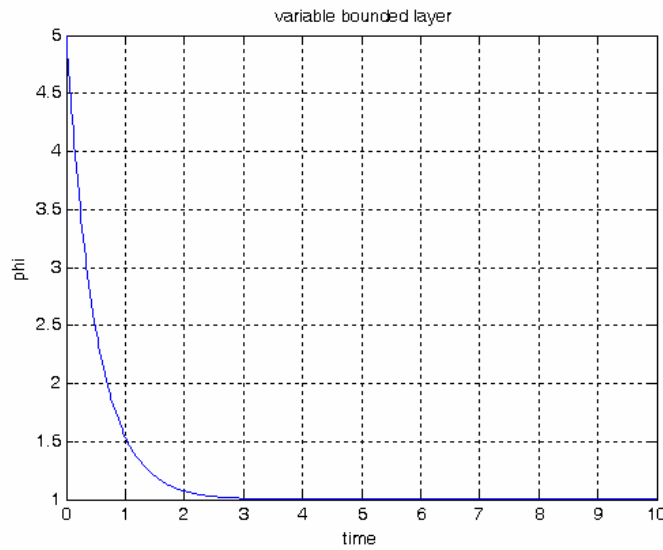


Figure 34. Profile of the Φ

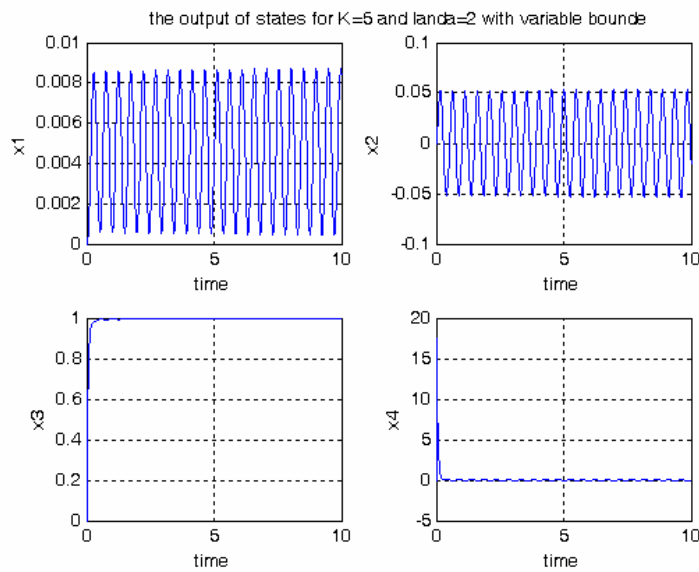
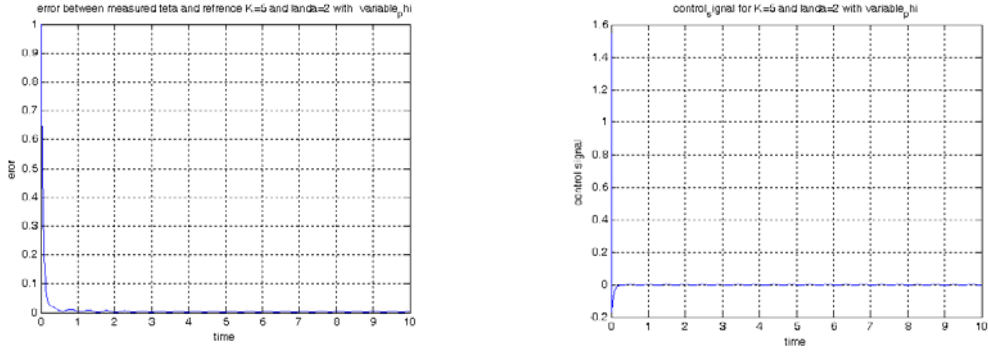


Figure 35. State variables with time varying soft switching sliding mode $\Phi = 10$, $k = 5$, $\lambda = 2$ و $y_{ref} = u(t)$



**Figure 36. time varying soft switching sliding mode $\Phi = 10$, $k = 5$, $\lambda = 2$, $y_{ref}=u(t)$
 (Left) Tracking Error (Right) Control Signal**

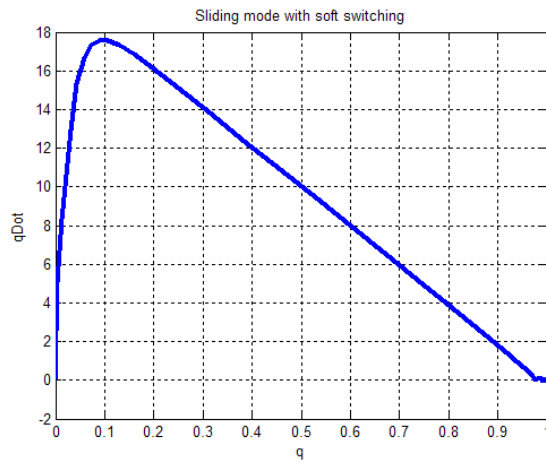


Figure 37. Phase portrait of sliding mode with time varying soft switching

3-7 Conclusion and comparison

In this section we briefly conclude our experiments in nonlinear control design on our benchmark problem. Table 6 presents overall comparison between the implemented nonlinear controllers.

1. Design complexity: The most tedious design belongs to the Input-State feedback linearization where the computation of control law was absolutely cumbersome. Designing the Backstepping controller was also a complex task due to the physical nature of the system. Sliding mode Control and Input-Output feedback linearization had simple systematic design rules.
2. Frequency Response Design Tools: Feedback linearization methods as a whole have good frequency representations, since they use a linearized system and it could be used for frequency response design very well. Sliding mode has explicit interpretation of frequency response of closed loop which could help designer to meet the requirement. But the Backstepping controller which a constructive Lyapunov controller lack explicit frequency analysis and all designer could do in this respect is to guaranty good convergence rate.
3. Min Actuator Saturation: actuator saturation is a significant practical constraint on controllers which is equivalent to cost and desirability of a nonlinear controller. Our results show that backstepping with more flexibility design could cause moderate or small control efforts. But the feedback linearization methods do the best in this field. However using sliding mode control without soft switching is nightmare in this respect. With soft switching, sliding mode also becomes to moderate spectrum.

4. CPU Usage: Feedback linearization method have lots of time cumsuming calculations and need more CPU resourse. Mean while backstepping has moderate CPU usage in run time and sliding mode is the fastest method since it uses a reduce representation of the system for control (1st order stabilization).
5. Performance: instead of Input-State poor performance we almost have good performance in all fields. The backstepping has be come slightly superior due to good design. However, creating a optimal backstepping system is a hard problem, but feedback linearization method provide simpler representations for seeking optimality. On the other hand, feedback linearization may eliminate some nonlinear terms in producing control law that if they were not eliminated the controller could have achieved a better performance [5].
6. Design Flexibility: The most flexible design procedure was backstepping with nice constructive Lyapunov structure. On the other hand, feedback linearization with poor rigid structure has almost no flexibility in nonlinear section. They have only degrees of freedom in linear section. Sliding mode has also a nice flexibility specially when it is incorporated with fuzzy system but it is not the case in our implementations.
7. Parameter Uncertainty Handling: Obviously, sliding mode as a robust method do the best in this field then backstepping with robust design could do a good job. Feedback linearization methods are model based system with little robustness in nonlinear design.
8. Unstructured Uncertainty Handling: Feedback linearization method are more worse here than parameter uncertainties. Sliding mode could do some nice job here but it is incorporated with dynamic soft

switching which varies with time. This field is backstepping reason of existence and it masters it.

Table 6. Overall comparison between the implemented nonlinear controllers

	Measure	Input-Output Feedback Linearization	Input-State Feedback Linearization	Backstepping	Sliding Mode
1.	Desing Complexity	+	-	-	+
2.	Frequecy Response Design Tools	+	+	-	+
3.	Min Actuator Saturation	+	+	Moderate	-
4.	CPU computation	- -	- -	Moderate	+
5.	Performance	+	-	++	+
6.	Design Flexibility	-	-	++	+
7.	Paramter Uncertainty Handling	Moderate	Moderate	+	++
8.	Unstructure Uncertainty Handling	-	-	++	+

References:

- [1] R. Kinsey, D. Mingori, and R. Rand, "Nonlinear controller to reduce resonance effects during despin of a dual-spin spacecraft through precession phase lock", Proceedings of the 31st Conference on Decision and Control, Arizona, USA, December 1992.
- [2] M. Tavakoli, H. D. Taghirad, and M. Abrishamchian, "Parametric and Nonparametric Identification and Robust Control of a Rotational/Translational Actuator", Proceedings of The Fourth International Conference on Control and Automation (ICCA'03), Montreal, Canada, 10-12 June 2003
- [3] Bupp RT, Bernstein DS, Coppola VT. A **benchmark problem for nonlinear control design: problem** statement, experimental testbed, and passive **nonlinear compensation**. [Conference Paper] *Proceedings of the 1995 American Control Conference (IEEE Cat. No.95CH35736)*. American Autom **Control Council**. Part vol.6, 1995, pp.4363-7 vol.6. Evanston, IL, USA.
- [4] Chih-Jian Wan, Bernstein DS, Coppola VT. **Global stabilization of the oscillating eccentric rotor**. [Conference Paper] *Proceedings of the 33rd IEEE Conference on Decision and Control (Cat. No.94CH3460-3)*. IEEE. Part vol.4, 1994, pp.4024-9 vol.4. New York, NY, USA.
- [5] Kokotovic P, Arcak M. **Constructive nonlinear control: a historical perspective**. [Journal Paper] *Automatica*, vol.37, no.5, May 2001, pp.637-62. Publisher: Elsevier, UK.
- [6] Jiayang Zhao, Kanellakopoulos I. **Flexible backstepping design for tracking and disturbance attenuation**. [Journal Paper] *International Journal of Robust & Nonlinear Control*, vol.8, no.4-5, 15-30 April 1998, pp.331-48. Publisher: Wiley, UK.
- [7] 5. Jankovic M, Fontaine D, Kokotovic PV. **TORA example: cascade- and passivity-based control designs**. [Journal Paper] *IEEE Transactions on Control Systems Technology*, vol.4, no.3, May 1996, pp.292-7. Publisher: IEEE, USA.
- [8] Kanellakopoulos I, Jiaxiana Zhao. **Tracking and disturbance rejection for the benchmark nonlinear control problem**. [Conference Paper] *Proceedings of the 1995 American Control Conference (IEEE Cat. No.95CH35736)*. American Autom **Control Council**. Part vol.6, 1995, pp.4360-2 vol.6. Evanston, IL, USA.
- [9] JJE Slotine and Weiping Li. *Applied nonlinear control*. Prentice Hall, Englewood Cliffs, NJ, 1991